

SUBMISSION UNDER 37 C.F.R. 41.37
IN THE UNITED STATES PATENT AND TRADEMARK OFFICE

In re Application of: Pais)	
Assignee: Dept of the Navy)	
Serial No.: 15/141,270)	Group Art Unit: 3644
Filed: 04/28/2016)	Examiner: Philip Bonzell
For: A Craft Using an Inertial Mass)	
Reduction Device)	Att. Docket No.: PAX 205
)	
)	

Commissioner of Patents and Trademarks
Washington, D.C. 20231

APPEAL BRIEF

Claims 1-4 (all of the claims) have been finally rejected, and the rejections of claims 1-4 are appealed herein. Final Rejection sent March 30, 2018, Advisory Action Before Filing of the Appeal sent July 11, 2018 stating application not in condition for allowance.

Table of Contents

i. Real Party in Interest.....	page 3
ii. Related Appeals, Interferences, and Trials.....	page 4
iii. Summary of Claimed Subject Matter.....	page 5
iv. Argument.....	page 6
v. Claims Appendix.....	page 16
vi. Evidence Appendix.....	page 17

I. REAL PARTY IN INTEREST

The real party in interested is the United States Government represented by the Secretary of the Navy (The Department of the Navy). The inventor is a U.S. government employee who invented the invention during the course of his employment. As a result, Federal law provides all rights to this invention belong to the United States of America under 37 C.F.R. 501.6.

II. RELATED APPEALS, INTERFERENCES AND TRIALS

There are currently no related appeals, interferences, and trials.

III. SUMMARY OF CLAIMED SUBJECT MATTER

The application contains four claims listed on page 17 of the specification. Claim 1 (lines 2-9 on page 17), the only independent claim of the application, is shown in Figures 1 and 2 and is described in paragraph 33, page 12 of the specification. Claim 1 describes a craft using an inertial mass reduction device 10. Claim 1 includes an inner resonant cavity wall 200, an outer resonant cavity wall 100, and microwave emitters 300. The inner resonant cavity wall 200 and the outer resonant cavity wall 100 form a resonant cavity 150. The microwave emitters 300 create high frequency electromagnetic waves 50 throughout the resonant cavity 150 causing the outer resonant cavity wall 100 to vibrate in an accelerated mode and create a local polarized vacuum 60 outside the outer resonant cavity wall 100.

IV. ARGUMENT

Rejection #1: Claims 1-4 under 35 USC 112(a)

Examiner rejected claims 1-4 under 35 USC 112(a) as failing to comply with the enablement requirement (in Examiner's Office Actions dated 11/28/2017 and 3/30/18). Examiner further stated that "the claims(s) contains subject matter which was not described in the specification in such a way as to enable one skilled in the art to which it pertains, or with which it is most nearly connected, to make and/or use the invention." He stated that "when referring to the specification as to ascertain about the microwave emitters needed in this system it is seen that for a high energy electromagnetic field to polarize a quantum vacuum as claimed it would take 10^9 [T]eslas and 10^{18} V/m." Examiner holds that these levels are not feasible with current technology and concludes that one skilled in the art could not make or use this invention.

The burden of proof is on the Patent Trademark Office to show unpatentability, not on the applicant to establish patentability, and "it remains on the PTO even if the [Examiner] has made a prima facie case" of inoperability. (*In re Rijckaert*, 9 F.3d 1531, 1532 (Fed. Cir 1993), *In re Oeriker*, 977 F.2d 1443, 1445 (Fed. Cir. 1992)). Furthermore, to establish a prima facie case of nonenablement, the Examiner "bears an initial burden of setting forth a reasonable explanation as to why [he or she] believes the scope of protection [sought in] that claim is not adequately enabled by the description of the invention provided in the" written description (*In re Wright*, 999 F.2d 1557, 1561-62 (Fed. Cir 1993), *In re Armbruster*, 512 F.2d 676, 677 (C.C.P.A. 1975)). The Examiner must "back up [these assertions] with acceptable evidence or reasoning" (*In re Marzocchi*

439 F.2d 220, 224 (C.C.P.A. 1971)). Furthermore, the Examiner must support rejections with references (*In re Vaack*, 947 F.2d 488, 495 (Fed. Cir. 1991)). A United States Court of Customs and Patent Appeals case held “a specification disclosure which contains a teaching of the manner and process of making and using the invention in terms which correspond in scope to those used in describing and defining the subject matter sought to be patented *must* be taken as in compliance with the enabling requirement of the first paragraph of § 112 *unless* there is reason to doubt the objective truth of the statements contained therein which must be relied on for enabling support.” (*Marzocchi*, 439 F.2d at 223 (C.C.P.A 1971)). In this case there is no reason to doubt the truth of the statements contained in the specification. The examiner must also explain any doubts as to the accuracy of any statement with evidence or reasoning rooted in fact (*Marzocchi*, 439 F.2d at 224 (C.C.P.A 1971)), and the PTO must provide a factual basis for an enablement rejection, rather than conclusory statements regarding the PHOSITA’s (person having ordinary skill in the art) level of skill (*In re Brebner*, 455 F.2d 1402, 1405 (C.C.P.A. 1972)). In this case, the Examiner did not utilize any references, provides no evidence as to accuracy or objective truthfulness of any statements, and makes a conclusion based on his personal knowledge.

Examiner stated that the declaration by Dr. James Sheehy, dated December 15, 2018 and filed January 23, 2018 (Sheehy Declaration #1), is insufficient to overcome the rejection based on 35 USC 112(a) and 112(b). In particular, the Examiner states on page 4, paragraph 6b, of his Final Rejection dated March 30, 2018, that because the inventor is funded and working on experiments does not provide proof of enablement. However, in a number of cases, the Court of Appeals for the Federal Circuit has held research plans and

proposals to be sufficiently enabled to be patentable on their own (*In re Montgomery*, 677 F.3d 1375, 1382 (Fed. Cir. 2012); *Eli Lilly & Co. v. Actavis Elizabeth LLC*, 435 F. App'x 917, 923-26 (Fed. Cir. 2011)). In particular, in *Allergan, Inc. v Sandoz, Inc.*, 796 F.3d 1293 (Fed. Cir. 2015), the Court stated that research plans enabled patents and quoted *Alcon Research Ltd. v. Barr Labs., Inc.*, 745 F.3d 1180, 1188 (Fed.Cir. 2014), “ ‘[a] patent does not need to guarantee that the invention works for a claim to be enabled.’” (*Alcon*, 745 F.3d at 1189).”

Enablement of Applicant's invention can also be found in two Applicant written, peer reviewed papers- AIAA 2017-5343 (Salvatore C. Pais. "A hybrid craft using an inertial mass modification device," *AIAA SPACE and Astronautics Forum and Exposition*, AIAA SPACE Forum) and SAE 2017-01-2040 (Salvatore Pais. "High Frequency Gravitational Waves - Induced Propulsion," SAE Technical Paper 2017-01-2040, 2017). As indicated in the Applicant's response dated January 23, 2018, paper SAE 2017-01-2040 states in the footnotes on the last page (page 5) as follows:

"The Engineering Meetings Board has approved this paper for publication. It has successfully completed SAE's peer review process under the supervision of the session organizer. This process requires a minimum of *three (3) reviews by industry experts.*" (Italics added for emphasis).

In response to Applicant's argument that the concept of the Application has been published by peer reviewed papers, Examiner stated in his March 30, 2018 Final Rejection, page 5, paragraph 7d, that "just because a concept was ... peer reviewed the concept does not equate to be patentable." It is important to note, that "peer reviews assess credibility, which is the degree of belief scientists attach to a research claim and

the facts presented to support it.” Peer reviewers are seen as “gatekeepers,” and ensure that the research claims are feasible (Frederick Grinnel, *Everyday Practice of Science* 75 (2009)). Peer review ensures that “each research claim is reproducible, logical, and independent and that it satisfies ... basic conditions for communal acceptance” (John Ziman, *Real Science* 246 (2002), Mark Erickson, *Science, Culture and Society* 44 (2004)). Peer reviewed work “is sent out to other scientists for criticism and judgement, only work judged as worthwhile will be published” (Gregory Derry, *What Science is and How it Works* 161 (1999)). In this case, the concept has been approved by two separate bodies (the American Institute of Aeronautics and Astronautics and SAE) deemed to be experts in their fields. Furthermore, “quantitative studies and anecdotal sources reveal reviewers resist change. They often reject anything that clashes with then-existing ideas and generally accepted theories.” (Sean Seymore, “Patently Possible.” *Vanderbilt Law Review*, Vol 54:5:1491 at 1509-1510). This further indicates that the concept is scientifically supported and feasible, and thus enabling as seen by the scientists or “gatekeepers” (who are persons of ordinary skill in the art) who reviewed the work.

Furthermore, the Examiner turned to *perceived* mainstream science to indicate the concept was not possible. However, in this matter, the gatekeepers of science (the peer reviewers of Applicant’s papers) indicated that the concept is possible and enabled. Furthermore, the Examiner is not an active researcher, and is not on the frontline of science, as the peer reviewers typically are. Thus, he is not aware of the current state of the art and is not a person of ordinary skill in the art of the subject matter of the Application.

Additionally, Applicant has filed a second declaration by James Sheehy, dated May 11, 2018, with the Second Amendment on May 24, 2018 (Sheehy Declaration #2). Dr. Sheehy's Declaration #2 indicated that the invention is enabled. Dr. Sheehy is the technical authority, and spokesperson for all basic, applied, advanced research and transition for the Naval Air Systems Command of the Department of Navy, and can be considered a subject matter expert and person of ordinary skill in the art. In Examiner's Advisory Action Before the Filing of an Appeal Brief, dated July 11, 2018, Examiner "held" that after considering the Sheehy declaration filed with Second Amendment "the claims are still not enabled." Examiner, however, agrees that high frequencies of vibration on the order of 10 Gigahertz are possible, by stating "obtaining high frequencies are possible." He further asks that the Applicant "demonstrate these high vibrational frequencies to create a local polarized vacuum." This directly contradicts the Federal Circuit's dicta that stated "[a] patent does not need to guarantee that the invention works for a claim to be enabled" (*Alcon*, 745 F.3d at 1189) and that it is improper for the Patent Office to suggest that an inventor had to offer proof for a claimed result (*In Re Cartwright*, 165 F.3d 1353 at 1359 (Fed. Cir. 1999)). Moreover, in Applicant's peer reviewed paper AIAA 2017-5343, it is shown that by vibrating electrically charged matter in an acceleration mode, it is possible to generate the high energy E-fields and B-fields that can polarize the vacuum. Thus, proving enablement of the invention.

Additionally, enablement is also shown in an IEEE paper (K.J. Coakley et al, "Estimation of Q-Factors and Resonant Frequencies" IEEE TRANSACTIONS ON MICROWAVE THEORY AND TECHNIQUES, Vol. 51, No. 3, March 2003), that Applicant described and entered into the record in his January 23, 2018 response to

Examiner's Office Action of November 28, 2017. The Examiner never addressed this reference or Applicant's arguments related to this reference, in any of his responses, that this paper shows enablement. The paper describes the fact that high Q-factors and vibrational frequencies in excess of 10 Gigahertz can be enabled readily. In particular, Table II on page 866 of this paper shows that by emitting microwaves within a copper resonant cavity it is possible to experimentally obtain vibrational frequencies in excess of 10 Gigahertz, thus enabling electromagnetic (EM) flux values of 10^{33} Watts/ m^2 , according to Equation 1 in the inventor's AIAA paper (AIAA 2017-5343). This EM flux value is equivalent to the generation of E-fields on the order 10^{18} V/m and B-fields on the order of 10^9 Tesla. Thus, the fields required for the invention are both feasible and enabled.

Thus, Claims 1-4 comply with the enablement requirement, and Examiner's rejection should be overturned.

Rejection #2: Claims 1-4 under 35 USC 112(b)

Examiner also rejected claims 1-4 under 35 U.S.C. 112(b) as being indefinite for failing to particularly point out and distinctly claim the subject matter the applicant regards the invention. Examiner states that "the amount of magnetic field and electricity required for the craft to 'work' are on the many of orders of magnitude beyond what can be created and as such it is not clear and therefore indefinite as to how this microwave emitter would provide the desired result."

Furthermore, the Examiner asserts in his Final Action dated March 30, 2018, Paragraph 7g that "there is no such thing as a repulsive EM energy field" and

“electromagnetism can be repulsive in certain circumstances, but there is no blanket field that repels everything.” This is incorrect, since it is well known by a person of ordinary skill in the art, that electromagnetic radiation fields are fields of photons which are *always* repulsive in action, since photons have no electrical charge, and act as carriers of energy and momentum. This is proved by the well-established physics of the Photoelectric Effect, whereby, photons over certain frequencies can emit electrons from a metal plate. This can be found in any undergraduate physics textbook, such as *Fundamental of Physics*, 8th Edition by Halliday and Resnick.

This indicates that the Examiner’s knowledge of what is physically possible is not on par with that of a subject matter expert in physics or a person of ordinary skill in the art.

Furthermore, a unanimous Supreme Court in *KSR Int’l Co. v Teleflex, Inc* (550 U.S. 398 (2007)) held that “a person of ordinary skill is also a person of ordinary creativity.” In this subject matter, the person of ordinary skill, due to the sophistication of the technology and subject matter, is someone with an advanced degree and years of work in the subject matter. Therefore, in this case a person of ordinary skill can fill any gaps in the Applicant’s disclosure from the peer reviewed articles and/or other sources. Thus, the subject matter the inventor regards his invention can be ascertained from publically available literature, particularly the aforementioned articles.

As discussed earlier, when a paper describing this invention was peer reviewed by subject matter experts, it was determined to be scientifically supported, feasible, and thus enabled. Furthermore, the Declaration by Dr. Sheehy indicates that it is clear to one skilled in the art how to enable the invention, thus the claims are not indefinite.

Moreover, recently, physicists have experimentally shown entanglement on a macroscopic scale, thus leading to macroscopic quantum coherence being feasible at high frequencies of vibration (*Nature Letters*, volume 556, pages 478–482 (April 25, 2018), in “Stabilized entanglement of massive mechanical oscillators,” authors C. F. Ockeloen-Korppi, E. Damskägg, J.-M. Pirkkalainen, M. Asjad, A. A. Clerk, F. Massel, M. J. Woolley & M. A. Sillanpää). This demonstrates that the physics required and described in the application and related AIAA technical paper by the inventor (AIAA 2017-5343) is correct, and not “just math theory,” as described by the Examiner in his March 30, 2018 Final Office action on page 4, paragraph 6a. Along these lines, on page 3 of the inventor’s AIAA 2017-5343 paper (described in January 23, 2018 Applicant’s Response), the inventor wrote:

“It is a well-known facet of quantum field theory that everything can be described in quantum mechanical terms. The complex interactions between a physical system and its surroundings (environment), disrupt the quantum mechanical nature of a system and render it classical under ordinary observation. This process is known as decoherence. However, it is argued that we can retard (delay) decoherence (and possibly even suppress it – namely decouple a physical system from the environment) by accelerated spin and/or accelerated vibration of electrically charged matter under rapid acceleration transients. This may be the very condition to achieve a state of macroscopic quantum coherence, the idea being that we never let the system achieve thermodynamic equilibrium, by constantly delaying the onset of relaxation to equilibrium (hence the production of maximal entropy is delayed). The system may “violently” react by generating

“anomalous” emergent phenomena, such as, but not limited to, inertial mass reduction.”

This further demonstrates that the invention is not “just math theory,” and the physical applicability of the inventive concept toward enablement. As discussed earlier, this paper was peer reviewed and thus can be deemed as accurate and scientifically correct.

Additionally, in a newly published international journal paper (“A smart power saving protocol for IoT with wireless energy harvesting Technique” by S. Madhurikkhal and R. Sabitha, *Cluster Computing* published March 16, 2018 by Springer, <https://doi.org/10.1007/s10586-018-2148-5>) in the field of Internet of Things (IoT) and Cluster Computing, one of Applicant’s paper (found in *Int. J. Space Science and Engineering*, Vol. 3, No. 4, 2015 and discussed in paragraph 19 of the specification) that describes how to enable the achievement of high energy electromagnetic fields is cited as a pioneering concept in Far-Field Wireless Power Transmission. Thus, indicating further evidence that subject matter experts (and people of ordinary skill in the art) state that such high energy electric and magnetic fields are feasible and can be created with current technology. As discussed earlier, the Coakley paper indicates that the fields required for the invention are feasible. Therefore, it is clear and not indefinite as to how the desired results would be obtained. Thus Examiner’s arguments and rejections are overcome.

Moreover, the fundamentally unique innovative principle of controlled motion of electrically charged matter (from solid to plasma) via accelerated spin and/or accelerated vibration under rapid acceleration transients, can result in high intensity electromagnetic energy flux, thereby resulting in novel energy harvesting and generation techniques and devices. Furthermore, this pioneering concept can result in the achievement of

Macroscopic Quantum Coherence, which translates to emerging technology breakthroughs in Tactical High Energy Lasers, Advanced Field Propulsion (hybrid aerospace craft and power plants), High Temperature (Room temperature) Superconductivity and Quantum Technologies, such as Spintronics and Quantum Computing.

In conclusion, Applicant's claims are enabled, feasible, and particularly point out and distinctly claim the subject matter the applicant regards as the invention. Thereby, all Examiner's rejections have been overcome, and the Claims 1-4 should be allowed.

V. CLAIMS APPENDIX

Status of Claims: All claims (Claims 1-4) received Final rejections.

Listing of Claims:

1. (original) A craft using an inertial mass reduction device comprising:
 - an inner resonant cavity wall;
 - an outer resonant cavity wall, the inner resonant cavity wall and the outer resonant cavity wall forming a resonant cavity; and,
 - microwave emitters such that the microwave emitters create high frequency electromagnetic waves throughout the resonant cavity causing the outer resonant cavity wall to vibrate in an accelerated mode and create a local polarized vacuum outside the outer resonant cavity wall.
2. (original) The craft of claim 1, wherein the resonant cavity is filled with a noble gas.
3. (original) The craft of claim 1, wherein the outer resonant cavity wall is electrically charged.
4. (original) The craft of claim 1, wherein the resonant cavity is axially rotated in an accelerated mode.

VI. EVIDENCE APPENDIX

1. Declaration of Dr. James Sheehy dated December 15, 2017 (Sheehy Declaration #1): entered into record the January 23, 2018.
2. Declaration of Dr. James Sheehy dated May 11, 2018 (Sheehy Declaration #2): entered into the record May 24, 2018.
3. Article AIAA 2017-5343: Salvatore C. Pais. "A hybrid craft using an inertial mass modification device," *AIAA SPACE and Astronautics Forum and Exposition*, AIAA SPACE Forum: entered into the record January 23, 2018.
4. Article SAE 2017-01-2040: Salvatore Pais. "High Frequency Gravitational Waves - Induced Propulsion," SAE Technical Paper 2017-01-2040, 2017: entered into the record January 23, 2018.
5. Article K.J. Coakley et al, "Estimation of Q-Factors and Resonant Frequencies." *IEEE TRANSACTIONS ON MICROWAVE THEORY AND TECHNIQUES*, Vol. 51, No. 3, March 2003) entered into the record January 23, 2018.

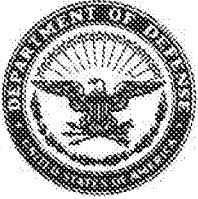
Appeal Brief for 15/141,270

Respectfully Submitted,

A handwritten signature in black ink, appearing to read "Mark O. Glut", written over a horizontal line.

Mark O. Glut
Registration #38,161
Department of the Navy
Office of Counsel, NAWCAD
47076 Liljencrantz Rd, Building 435
Patuxent River, MD 20670-1547
(301) 757-0582

Date: August 16, 2018



DEPARTMENT OF THE NAVY

NAVAL AIR SYSTEMS COMMAND
RADM WILLIAM A. MOFFETT BUILDING
47123 BUSE ROAD, BLDG 2272
PATUXENT RIVER, MARYLAND 20670-1547

IN REPLY REFER TO

5216
Ser 40T/33
15 Dec 2017

From: Naval Aviation Enterprise (NAE) Chief Technology Officer (CTO), AIR 4.0T
To: Mr. Philip J. Bonzell, Primary Patent Examiner, USTPO
Subj: U.S. Patent Application 15/141,270 (PAX 205)

1. Mr. Bonzell, Dr Pais has shared your review of his patent disclosure and I agree with your main point that this mode of acceleration / movement is beyond the state of the possible, at least at present. If you understand the theory and follow the equations you do arrive at the same conclusion or supposition as Dr. Pais. It is clear from your review that you did invest the time and did follow the theory. As you well know everything with time, if of significance, which this certainly is grows in power / magnitude. The theory which led to the first ruby laser in 1960 is a perfect example. With time lasers have evolved into a myriad of different wavelengths, power, and pulse durations. In 1960 1 CW watt at 695nm was a landmark, while now a kJ at up to pico / atosecond pulse is not uncommon and is ever increasing expanding the potential usages. At the time Hughes claimed the invention while actually the Army at Picatinny Arsenal had built the first ruby laser in 1958 but never sought a patent much to DoD's loss.

2. In U.S. Patent Application 15/141,270 (PAX 205) we are looking at very much the same phenomena. Dr. Pais is currently funded by NAWCAD to design a test article and instrumentation to demonstrate the experimental feasibility of achieving high electromagnetic (EM) field-energy and flux values (Watts/meter²). He is currently one year into the project and has already begun a series of experiments to design and demonstrate advanced High energy Density / High Power propulsion systems.

3. Dr. Pais' approach of reaching this objective is to couple an electrically charged system's high frequency axial spin with high vibration frequencies operated in a rapidly accelerated transient mode to achieve extremely high electromagnetic field-intensities (EM energy flux), which as you understand is the equivalent of achieving extremely high E- and B-fields. If successful the realization of this result demonstrates that this patent documents the future state of the possible and moves propulsion technology beyond gas dynamic systems to field-induced propulsion based hybrid aerospace-undersea craft.

4. Dr. Pais is currently performing tests using a battery to charge a 10 cm test sample spinning at up to 100,000 RPM and is able maintain charge on these batteries for dwell times of more than 25 minutes (at max RPM) without loss of load. If the desired results are not achieved due to the sample's charge, then he will move to using a super-capacitor as the spinning test asset. With test asset surface charge density on the order of one Coulomb/meter², we expect to see high EM energy flux amplification as we accelerate the spin of the test asset up to 100,000 RPM, subjecting the test asset to several rapid acceleration transients.

5. Based on these initial findings I would assert this will become a reality. China is already investing significantly in this area and I would prefer we hold the patent as opposed to paying forever more to use this revolutionary technology. Please contact me if you would like to discuss further or have questions. I appreciate your time and thorough review.

Dr. JAMES SHEEHY

DECLARATION UNDER 37 C.F.R. 1.132

IN THE UNITED STATES PATENT AND TRADEMARK OFFICE

In re Application of: Pais)	
Serial No.: 15/141,270)	Group Art Unit: 3644
Filed: 04/28/2016)	Examiner: Philip Bonzell
For: A Craft Using an Inertial Mass)	
Reduction Device)	Att. Docket No.: PAX 205
)	

Commissioner of Patents and Trademarks
Washington, D.C. 20231

DECLARATION UNDER RULE 1.132

I, James Sheehy, declare and say as follows:

That I received a Doctor of Philosophy Degree (PhD) in physiological optics from the Pennsylvania State University, a Master's degree from the Rensselaer Polytechnic University in Human Factors Engineering (with research performed in energy efficient vehicles), and a Bachelor's degree from Kean University.

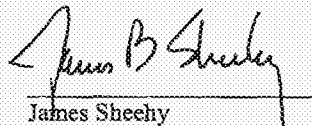
That I have served as a civilian employee of the United States Navy since 1985. During the course of my career at the Department of the Navy, I was a research and lab manager, and the Chief Scientist of the Naval Air Systems Command. I have directed all basic to advanced technology research while continuing to pursue research interests in perception, physiological optics, visual vestibular interactions, analog then digital sensors and displays for night vision / low light level devices, nonlinear materials and novel coatings for filters and lenses. As a result, I am well versed in the generation of electromagnetic fields and in physics in general (the subject matter of the above application).

That for the past eleven years I have been and am currently the Chief Technology Officer of the Naval Aviation Enterprise, and NAVAIR's Chief Scientist/CTO and technical authority, and spokesperson for all basic, applied, advanced research and transition. I was promoted to the Senior Executive Service in November 2001 and was awarded the Presidential Rank Award for sustained superior accomplishments in 2007.

That I am familiar with the above referenced patent application (and related amendment), as well as the development, usage and properties of the craft using an inertial mass reduction device. That as a result of my education and career, I am regarded as a subject matter expert and can be considered "a person of ordinary skill in the art" in the subject matter of the above patent application.

That the invention described in the above referenced patent application is enabled via the physics described in the patent application and the peer reviewed papers described in the Inventor Amendment dated January 23, 2018.

That I declare that all statements made herein of my own knowledge are true and that all statements made on information and belief are believed to be true; and further that these statements were made with the knowledge that willful false statements and the like so made are punishable by fine or imprisonment, or both, under 18 USC 1001.


James Sheehy

May 11, 2018



A Hybrid Craft using an Inertial Mass Modification Device

Salvatore Cezar Pais¹

Department of the Navy, NAVAIR/NAWCAD, NAS Patuxent River, MD. 20670

It is possible to envision a hybrid aerospace-undersea craft (HAUC), which due to the physical mechanisms enabled with an inertial mass reduction device, can function as a submersible craft capable of extreme underwater speeds (lack of water-skin friction due to electromagnetic field-induced water molecules repulsion) and enhanced stealth capabilities (non-linear scattering of radio frequency and sonar signals). This hybrid craft would move with ease through the air, space, water mediums, by being enclosed in a bubble (shield), generated due to the coupled effects of electromagnetic field induced air/water particles repulsion and vacuum energy polarization. Moreover, it may be possible to reduce the inertial mass of a system/object in motion, by applied high energy electromagnetic fields, achieved by a novel coupling of accelerated high frequency vibration with accelerated spin of electrically charged matter in close proximity to the system/object in question. This original method of accelerated spin/accelerated vibration of charged matter would be executed under rapid acceleration transients for maximum effect. The resultant high energy flux (on the order of 10^{33} Watts/m²) when concentrated in a small area around the contour of the object (craft) can generate energy densities of 10^{25} Joules/m³, commensurate with Schwinger electric field values for vacuum polarization. As a result, extreme craft speeds can be achieved, thus enabling a novel method of advanced propulsion.

I. Introduction

The original concept described herein, gives rise to the design of an inertial mass reduction device (IMRD) and materializes into the hybrid aerospace-undersea craft (HAUC). When put in practice, this system can lead to the design of energy generation machinery with power output levels much higher than those currently achievable. The utilization of such high power sources for space power and propulsion generation, as it pertains to reduction in a hybrid craft's inertial mass as a direct result of local vacuum polarization, is an important application of the described theoretical concept.

This concept's governing physics teaches that it may be possible to reduce the inertial mass of a system/object in motion, by applied high energy electromagnetic (EM) fields, achieved by coupling of accelerated high frequency vibration with accelerated spin of electrically charged matter in close proximity to the system/object in question. This original method of accelerated spin and/or accelerated vibration of electrically charged matter would be executed under rapid acceleration transients for maximum effect.

There are four known fundamental forces which control matter and therefore control energy, namely the strong and weak nuclear forces, the electromagnetic force and the gravitational force. In this hierarchy of forces, the electromagnetic force is perfectly positioned to be able to manipulate the other three. A stationary electric charge gives rise to an electric (electrostatic) field, while a moving charge generates both an electric and a magnetic field (hence the electromagnetic field); additionally an accelerating charge induces electromagnetic radiation in the form of transverse waves, namely light. Mathematically as well as physically, electromagnetic field energy flux can be represented as the product of electric field strength and magnetic field strength. Electromagnetic fields act as carriers for both energy and momentum, thus interacting with physical entities at the most fundamental level.

Artificially generated, high energy, electromagnetic fields interact strongly with the vacuum energy state, an aggregate/collective state comprised of the superposition of all quantum fields' fluctuations permeating the spacetime continuum [1]. According to quantum field theory, this strong interaction between the fields is based on the mechanism of transfer of vibrational energy between the fields, further inducing local fluctuations in adjacent quantum fields which permeate spacetime. These fields may or may not be electromagnetic in nature [2]. Matter, energy and spacetime are emergent constructs which arise out of a fundamental framework, the foundational structure that is the vacuum, energy state.

¹ Aerospace Engineer, NAWCAD Air 4.3.5.1, B. 2187 NAS Patuxent River, MD. 20670 - AIAA member

Everything that surrounds us, ourselves included, can be described as macroscopic collections of fluctuations, vibrations, oscillations in quantum mechanical fields. Matter is confined energy, bound within fields, frozen in a quantum of time. Therefore, under certain conditions, such as the coupling of high frequency axial spin with high frequency vibrations of electrically charged systems, the rules and special effects of quantum field behavior also apply to macroscopic physical entities [3].

Consider that we are immersed in an ocean of energy, the vacuum energy state, yet ordinarily we seem not to interact with it. This is because under normal circumstances (at or near equilibrium), the vacuum state is homogeneous, isotropic, Lorentz invariant, in other words it is symmetric. Break this symmetry (far-from-equilibrium), and strong interactions with the vacuum energy state become possible, thus affecting the manner in which the collective fields exchange energy with one another.

If we perform a “gedankenexperiment” we observe that the coupling of high frequency spin with high frequency vibration, especially for rapidly accelerated spin/vibration of an electrically charged system (object) puts every point on the boundary of the object in a state of coherent superposition, thereby inducing a macroscopic quantum phenomenon [4].

Moreover, as observed from the Casimir effect, the boundary conditions of a physical system affect the local vacuum energy state (VES) of that system (comprised of zero point EM energy (QED) among other types of field energies (QCD, Higgs, etc.)) thereby affecting the system’s physical properties [1]. Thus by manipulating/modifying the boundary conditions of a physical system with respect to its local VES (local quantum vacuum), we can alter the system’s physical properties.

Investigation of the quantum vacuum as a source of propulsion estimated the very short scales of time and distance (and hence the high energies) over which the quantum vacuum must be interacted with for extracting enough propulsive energy for relativistic interstellar flight. Based on this investigation, it was suggested that a system’s inertia may be a consequence of quantum vacuum electromagnetic behaviour, therefore by polarizing the vacuum in the proximity of the system, inertial mass reduction may be achieved [5-9].

Polarization of the local vacuum energy state is analogous to manipulation/modification of the local spacetime energy density, so as to reduce the resistance to motion of a propagating craft. As a result, extreme craft speeds can be achieved, thus enabling a novel method of advanced propulsion.

II. High Energy Electromagnetic Flux Generation

As originally observed in reference 4, for conditions of accelerated vibration or accelerated spin of an electrically charged object/system, we can write for the maximum EM energy flux (time rate of change of EM energy transfer per unit surface area):

$$S_{\max} = f_G (\sigma^2 / \epsilon_0) [(R_v v^2) t_{\text{op}}] \quad (1)$$

, where f_G is the charged system geometric shape factor (equal to 1 for a disc configuration), σ is the surface charge density, ϵ_0 is the electrical permittivity of free space, R_v is the vibration (harmonic oscillation) amplitude, v is the angular frequency of vibration in Hertz, and similarly in the case of axial spin R_v is the effective system radius, while v represents the angular frequency of rotation, and t_{op} is the operational time for which the electrically charged system is operated at maximum acceleration ($R_v v^2$). This closed form formulation is the result of the synthesis of classical electromagnetic field theory with the physics of simple harmonic motion.

Furthermore, for the case of rapid time rates of change of accelerated vibration / spin (rapid acceleration transients) of the charged system, given that the time differential of acceleration is non-zero, we obtain:

$$S_{\max} = f_G (\sigma^2 / \epsilon_0) [(R_v v^3) t_{\text{op}}^2] \quad (2)$$

This is a thought provoking formulation because it shows that even with moderate vibrational / spin frequencies in a rapidly accelerating mode, the EM energy flux is greatly amplified.

Thus if the product of all the controllable parameters in equation 2 (other than the angular frequency of vibration) was of unit order, we can achieve energy flux values on the order of 10^{33} W/m² (endemic of the polarized vacuum energy state) with low end microwave frequencies on the order of 10^7 Hz , inducing vibrations of a resonant

cavity wall of equal or higher frequencies, depending on cavity material. This in itself may qualify as an interesting observation, showing the extensive capabilities of a high energy / high frequency electromagnetic field generator.

Furthermore if we consider adding to the equation representing simple harmonic motion an “energy/momentum-pumping” (negative damping) term (bv), endemic of system acceleration, where b is a constant and v is (dx/dt) , namely the speed of a vibrating mass (m), something interesting occurs, in that it can be shown that the maximum of the total energy (E_T) of the vibrating system can be written as:

$$E_T \approx m R_v^2 \Omega^2 [\exp(2 \Omega t)] \quad (3)$$

, where Ω is the angular frequency of vibration, under the condition $[\Omega = (b/2m) \gg \Omega_0$ (natural frequency of vibration)]. Since the EM energy flux is directly proportional to E_T , we observe that there will be exponential growth in energy flux with accelerating vibration, especially under the condition of rapid acceleration transients.

Considering a classical Newtonian second law expression using the Lorentz (EM) force, we can relate the vibrating mass (m) with its vibrating charge (Q), in that m becomes directly proportional to the square of the ratio (Q/Ω). Coupling this relation with equation 3 yields:

$$S_{\max} \approx (Q^2 / \epsilon_0) (R_v^2 / R_s^5) \Omega [\exp(2 \Omega t)] \quad (4)$$

Equation 4 represents the maximum EM flux that can be achieved by accelerated vibration under the aforementioned condition, and applies to a spherical geometry (radius R_s) for a vibrating mass (m) of corresponding charge (Q).

The resultant high energy EM flux, on the order of 10^{33} Watts/m², and possibly much higher, when concentrated in a small area around the contour of the object (craft) can generate energy densities of 10^{25} Joules/m³, commensurate with Schwinger electric field values for vacuum polarization [9,10]. This physical condition is representative of the QED vacuum breakdown and is indicative of possible inertia control by altering the local vacuum energy density [1].

If we consider cosmic space as a superfluid medium [11], we may be able to say that the IMRD device has the capability of inducing a local phase transition from a turbulent regime to a laminar regime, thus allowing for “smooth sailing” of a hybrid craft (HAUC) through the specially conditioned vacuum of Space. This is a vacuum that has undergone macroscopic quantum coherence, locally, around the craft. As a result, the craft experiences “suction” into the conditioned vacuum.

It is a well-known facet of quantum field theory that everything can be described in quantum mechanical terms. The complex interactions between a physical system and its surroundings (environment), disrupt the quantum mechanical nature of a system and render it classical under ordinary observation. This process is known as decoherence [3].

However, it is argued that we can retard (delay) decoherence (and possibly even suppress it – namely decouple a physical system from the environment) by accelerated spin and/or accelerated vibration of electrically charged matter under rapid acceleration transients.

This may be the very condition to achieve a state of macroscopic quantum coherence, the idea being that we never let the system achieve thermodynamic equilibrium, by constantly delaying the onset of relaxation to equilibrium (hence the production of maximal entropy is delayed). The system may “violently” react by generating “anomalous” emergent phenomena, such as, but not limited to, inertial mass reduction.

Enter the Prigogine effect, as described in reference 4, on page 316.

The Prigogine effect teaches us that depending on three conditions, a chaotic system, namely the ‘soup’ of fluctuations that make up the vacuum energy state, can self-organize into an orderly state, equivalent to the state of macroscopic quantum coherence.

These conditions are the existence of a highly non-linear medium (the cosmic superfluid), an abrupt departure far-from-thermodynamic equilibrium (the accelerated spin/vibration of charged matter) and last but not least an energy flux (the generated EM energy flux) to maintain the process of self-organization (order from chaos).

All three conditions for the Prigogine effect are met in our application, thus it can be argued that a possible theoretical path toward inertial mass reduction induced by macroscopic quantum coherence is herein established.

III. Possible Mathematical Formalism of Inertial Mass Reduction

Consider that it may be possible to reduce the inertial mass and hence the gravitational mass (based on the Equivalence Principle), of a system/object in motion, by an abrupt perturbation of the non-linear background of local Spacetime (the local Vacuum energy state). This abrupt perturbation is equivalent to an accelerated departure far from thermodynamic equilibrium, analogous with Symmetry-breaking induced by abrupt changes of state (structure).

Moreover, it is possible to argue that gravitational (inertial) mass reduction is feasible by high frequency accelerated axial rotation (spin) and/or accelerated high frequency vibration of possibly charged objects, within the context of non-equilibrium thermodynamics.

In a published Physical Review Letter [12], Hayasaka and Takeuchi report the anomalous weight reduction of gyroscopes for right rotations only. At the time, the authors could not elucidate the physics behind these anomalous results. Several null result experiments followed [13-15], which declared the Hayasaka et al. results null and void, or at least questionable.

As described in Ref. 13, there were several differences between refs. 14 and 15 with respect to ref. 12, chief among these being the gyroscopes were spun in closed but not evacuated containers. Furthermore, the rotors were air driven rather than electrically driven, which may result in experimental inaccuracies. The main experimental set-up difference between ref. 12 and ref. 13 is that the pressure range within the vacuum container in the Hayasaka et al. experiment was reported as 1.3×10^{-2} Pa to 1.3 Pa while the Nitschke et al. experiment reported a pressure range of 1 – 3 Pa in the evacuated container. Moreover, refs. 13 - 15 experiments did not use the same gyroscope assemblies as used in ref. 12, nor the same experimental set-up as shown in figure 1 of the Hayasaka et al. work. It can be argued that exact replication of the experimental set-up and gyro-rotational acceleration procedure used in the anomalous weight reduction experiment was not achieved by any of the null result experiments. Two more relatively recent experimental attempts at nullifying the Hayasaka et al. experiment have been made [16, 17]. These attempts also do not correctly reproduce it (both experimental set-up and procedure), namely ref. 16 performs the experiment with free-falling rotating gyroscopes, while ref. 17 performs the experiment in a sealed environment only, without an evacuated test chamber.

It is important to note that in the Hayasaka et al. experiment, the gyro-rotor was electrically spun, which means there could have been an electrical charge on the rotor, however small, yet strong enough to possibly repel the air molecules close enough to the rotor (as shown in their figure 1) thus generating the negative pressure effect which possibly produced the anomalies observed.

In other words, the existence of a charge on the rotor, could have generated an EM energy flux strong enough to produce an ultrahigh vacuum condition in close proximity to the rotor, endemic of the quantum vacuum state (air particles' repulsion coupled with possible Vacuum polarization).

This can be possible when considering the idea that controlled motion (either by accelerated vibration and/or accelerated spin) of charged matter under rapid acceleration transients can induce macroscopic quantum coherence, locally.

Closer attention to the non-zero intercept of the Hayasaka et al. expression relating the gyro's weight diminution with respect to its mass, its angular rotational frequency and its effective rotor radius, yields the possibility of a local quantum Vacuum effect, namely a negative pressure (repulsive gravity) condition being present. This is due to the non-zero intercept being of the same order of magnitude with the Fokker-Planck electron-proton thermal equilibration rate, given an approximate Hydrogen atom number density of 40 atoms/m^3 , commensurate with the local Vacuum state.

Consider the Hayasaka et al. expression for gyro-weight reduction, written in SI units as:

$$\Delta W_R(\omega) = -2 \times 10^{-10} M r_{eq} \omega \text{ (kg m s}^{-2}\text{)} \quad (5)$$

, where ΔW_R is the reduction in weight, M is the mass of the rotor (in kg), ω is the angular frequency of rotation (in rad/s), and r_{eq} is the equivalent gyro-radius (in m).

From this relationship we see that the units of the non-zero intercept (2×10^{-10}) are (1/s).

This non-zero intercept is endemic of the physics of gyro-rotational acceleration, as follows.

It is possible to argue that as the gyro-rotor accelerates in its rotation, there is an abrupt departure far from thermodynamic equilibrium (within the evacuated container), given the high limit of angular rotational frequency of $1.3 \times 10^4 \text{ rpm}$.

Recall that the Hayasaka et al experiments were performed at room temperature (approximately 300 °K). Hypothetically speaking, we can think of the air particles within the evacuated container as giving rise to a non-thermal plasma (any plasma which is not in thermodynamic equilibrium because the velocity distribution of one of the species does not follow a Maxwell-Boltzmann distribution), formed when the matter inside the evacuated container is driven far from thermal equilibrium by the abrupt gyro-rotor acceleration. The system will now try to reach thermal equilibrium and this will be dependent on the electron-proton thermal equilibration rate.

Recall from plasma physics [18], that Coulomb collisions between the plasma's electrons and protons will in time (once the gyro-acceleration has ceased) force the particles to randomly exchange energy, and thus drive them into thermal equilibrium. Thus, in time the particles will equilibrate at the room temperature at which the experiment was conducted (assuming a non-Maxwellian velocity distribution).

Using the Fokker-Planck formulation for the electron-proton thermal equilibration rate (f_{ep}) with units of (1/s), we can write:

$$f_{ep} = (2n\sigma_T \ln\Lambda / \pi^{1/2}) (m_e / m_p) (k_B T_e / m_e c^2)^{-3/2} = 4 \times 10^{-8} (n / 1 \text{ m}^{-3}) (T_e / 1 \text{ eV})^{-3/2} (\ln\Lambda / 10) (\text{s}^{-1}) \quad (6)$$

, where n is the Hydrogen atom number density, σ_T is the Thompson cross-section (which equals $6.65 \times 10^{-29} \text{ m}^2$), $\ln\Lambda$ is the Coulomb logarithm (we set this at 10 to counteract its effect since this is a non-thermal plasma), T_e is the temperature at which the electrons and protons will equilibrate (approximately 300 °K).

Using a (n) value of 40 atoms/ m^3 , which is commensurate with the density of matter in the Vacuum (approx. $7 \times 10^{-29} \text{ g/cm}^3$), we obtain a thermal equilibration rate on the order of 10^{-10} (1/s) .

In light of this result, we can affirm that the non-zero intercept in the Hayasaka et al. gyro-weight reduction expression has the same order of magnitude as the thermal equilibration rate, thus matching the physics described above.

Leaving aside the inconsistency between the Vacuum of General Relativity and that of relativistic quantum field theory (best expressed by the Cosmological Constant discrepancy), the Vacuum's energy density is characterized by a negative pressure, and thus a repulsive gravity, which would explain the gyro-weight reduction effect, if indeed the local Vacuum state is achieved. We define the local Vacuum state as the macroscopic aggregate /collective state comprised of the superposition of all fluctuations in the quantum fields that permeate local spacetime.

Furthermore, we can assert that since the thermal equilibration rate is a function of the inverse temperature (raised to the 3/2 power) at which thermal equilibrium is re-established, if we were to cryogenically cool the gyro-rotor (which could be made from a superconducting material) to a temperature of $(10^{-3}) \text{ } ^\circ\text{K}$ (or below) we would obtain further reduction in the gyro-weight, if the Hayasaka et al result holds valid.

As an aside, we can hypothesize that if the gyro-rotor was to vibrate uniformly (instead of rotating), and its vibration (harmonic oscillation) was to accelerate in frequency (thus inducing a state of abrupt departure from thermodynamic equilibrium), it is possible that the resulting physics would be the same as that describing the rotational acceleration, thus we may write (using a simple dimensional analysis):

$$\Delta W_R (v) = - f_{ep} M A_v v \text{ (kg m s}^{-2}\text{)} \quad (7)$$

, where f_{ep} is the thermal equilibration rate, A_v is the vibration amplitude and v is frequency of vibration (in 1/s).

It is true though, that the presented hypothesis on the possible equality between the Hayasaka et al. non-zero intercept and the thermal equilibration rate (which is related to the electron-proton collision frequency) does not explain why the gyro-weight reduction only occurs in the right rotation mode (since the abrupt excursion from thermodynamic equilibrium caused by the gyro-rotor's rotational acceleration should occur for left rotations as well).

Due to this inconsistency (in addition to the non-zero intercept explanation as the thermal equilibration rate), as well as the lack of exact replication of the Hayasaka et al. experiment (both set-up and procedural aspects), further investigation into the reproducibility of this experiment is in demand, which if verified/validated has important implications in the advancement of foundational physics.

In view of the described physics, it is suggested that the Hayasaka et al. experiment be executed under the following conditions: a pressure of 10^{-4} to 10^{-2} Pa in the evacuated chamber, a gyro-spin frequency range of 1.3×10^4 to 10^5 rpm , and most importantly, under high rates of change of rotational and vibrational acceleration (to ensure abrupt departure far from equilibrium). It is further suggested, that the gyro-rotor be electrically charged, with at least a unit order surface charge density. Moreover, execute the transient ramping up-down-up of the rotor charge.

The results of these proposed experiments would greatly benefit new advancements in Aerospace Propulsion (conducive to Intergalactic Spaceflight), since it would show that it is possible to reduce the inertial mass, and hence the gravitational mass, of a system/object in motion, by an abrupt perturbation of the non-linear background of local Spacetime, equivalent to an accelerated departure far from thermodynamic equilibrium, analogous with Symmetry-breaking induced by abrupt changes of state / phase transitions. As a result, extreme speeds can be achieved.

IV. Enablement of HAUC Concept

The coupling of high spin frequency with high vibration frequency in order to achieve the desired inertial (gravitational) mass reduction effect, can lead to the design of an Inertial Mass Reduction Device (IMRD), shown in figure 1 in a hybrid aerospace/underwater craft (HAUC) configuration. This device utilizes microwave-induced vibration within a resonant annular cavity. The manner and effectiveness with which the microwave energy couples with the resonant cavity inner wall is called the cavity Q-factor. This parameter can be written as the (Energy stored / Energy lost) ratio and is in the range of 10^4 to 10^9 (and beyond), depending on whether ordinary metal (Aluminum or Copper at room temperature) or cryogenically cooled superconducting material (Yttrium Barium Copper Oxide or Niobium Germanium) is used for the resonant cavity inner wall and outside mold line skin of the aerospace vehicle. One must realize that the high energy/high frequency electromagnetic field generator responsible for the inertial mass diminution effect would generate a repulsive EM energy field while in earth's atmosphere, thereby repelling air molecules in its path of ascent/flight. Consequently, once in orbital space, by local Vacuum polarization (quantum field fluctuations' modification), a repulsive gravity effect (recall the negative pressure of the polarized Vacuum condition) would permit swift movement of the hybrid craft (which comes in either a cone or lenticular triangle /delta wing configurations), beyond our Solar System. A plurality of microwave antennas (high radio frequency emitter sources) in the electromagnetic (EM) spectrum range of 300 Megahertz to 300 Gigahertz are arranged within the annular duct - resonant cavity (surrounding the crew compartment and powerplant system, which would be guarded in a Faraday-type cage, against all EM radiation effects), as portrayed in figure 2. An auxiliary propulsion unit (not shown), would provide the initial aerospace/undersea hybrid vehicle thrust and electrical power generation. Furthermore, if the annular resonant cavity duct is filled with a noble gas such as Xenon (inert), the microwave energy collision with the gas particles will induce a plasma state of matter (further augmenting the oscillatory vibrations experienced by the resonant cavity inner wall), thereby creating a highly non-linear environment (phase transitions / abrupt changes of state from gas to plasma, which induce symmetry breaking) which will intensify the Prigogine effect (order from chaos - reference 4). This will enable the coherence of quantum vacuum fluctuations in the proximity of the outside mold line skin (electrically charged) of the aerospace vehicle, in this manner assuring a high degree of vacuum polarization.

Therefore, it is possible to envision a hybrid aerospace / undersea craft (HAUC), which due to the physical mechanisms enabled with the IMRD, can function as a submersible craft capable of extreme underwater speeds (lack of water-skin friction) and enhanced stealth capabilities (non-linear scattering of RF and sonar signals). This hybrid craft would move with great ease through the air/space/water mediums, by being enclosed in a Vacuum plasma bubble/sheath, due to the coupled effects of EM field-induced air/water particles repulsion and Vacuum energy polarization.

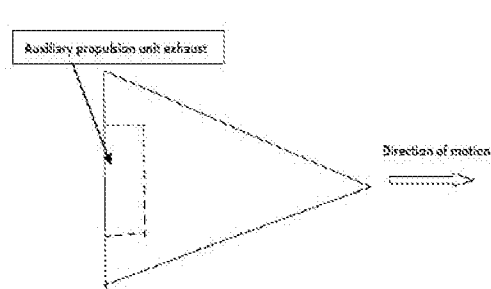


Figure 1. Hybrid Aerospace/Undersea Craft (HAUC) configuration

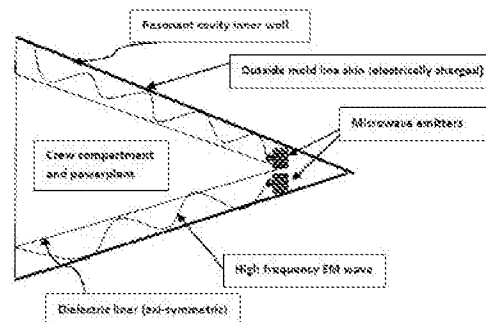


Figure 2. IMRD - Microwave Emitter configuration (Cross-sectional side view)

V. Conclusion

The original concept presented in this paper, suggests that it is possible to design a hybrid craft which by delivering vast amounts of electromagnetic energy flux in its close proximity can alter the spacetime energy density in that locality. In this manner, the craft can move at extreme speeds, due to quantum electrodynamic Vacuum breakdown effects, which result in inertial mass reduction. In parallel, controlled motion of electrically charged matter under accelerated vibration and/or accelerated spin and subjected to rapid acceleration-deceleration-acceleration transients, can be used in conjunction with nested EM fields (EM fields within EM fields) and the enablement of the Gertsenshtein effect, in order to manipulate / modify gravitational fields for propulsion, or to provide novel methods of plasma confinement and compression for nuclear fusion research.

Moreover, it is important to note that the extremely high EM energy flux magnitudes achieved with the concept at hand can be used in the design of space systems which could deflect, re-direct and/or destroy asteroids, such as Apophis (99942), on possibly dangerous trajectories close to Earth in 2029 and 2036. Such a system is the subject of US Patent Application number US 2017/0025935 A1, titled "Electromagnetic Field Generator and Method to Generate an Electromagnetic Field".

Acknowledgments

Funding for this work was provided by the Naval Innovative Science & Engineering (NISE) --Basic & Applied Research (BAR) program, under the project name "The High Energy Electromagnetic Field Generator (HEEMFG)", project number 219BAR-17-009. I wish to thank Dr. James Sheehy, Chief Technology Officer, Naval Aviation Enterprise, for the many hours of thought-provoking discussions on the concept at hand.

References

1. M. Millis and E. Davis, *Frontiers of propulsion science*, AIAA Progress in Astronautics and Aeronautics, Vol. 227, pp 199-201, 404, 2008.
2. J. Rafelski and B. Muller, *The structured vacuum*, Verlag Harri Deutsch, 1985.
3. A.D. O'Connell et al., Quantum ground state and single-phonon control of a mechanical resonator, *Nature* **464**, 697-703, April 1, 2010
4. S.C. Pais, The high energy electromagnetic field generator, *Int. J. Space Science and Engineering*, Vol.3, No. 4, 2015 pp.312-317.
5. B. Haisch, A. Rueda and H.E. Puthoff, Inertia as a zero-point field Lorentz force, *Phys. Rev. A* **49**, 678 (1994)
6. H.E Puthoff, Polarizable-Vacuum (PV) Approach to General Relativity, *Foundations of Physics*, Vol. 32, No.6, June 2002
7. H.E. Puthoff, Advanced space propulsion based on vacuum (spacetime metric) engineering, *JBIS*, Vol. 63, pp 82-89, 2010.
8. H.D. Froming, Quantum vacuum engineering for power and propulsion from the energetics of space, presented at the Third International Conference on future Energy, Washington D.C. October 9-10, 2009.
9. J. Schwinger, 1951 *Phys. Rev.* **82** 664.
10. S.P. Kim, On Vacuum Polarization and Schwinger pair production in intense lasers, 23rd International Laser Physics Workshop (LPHYS'14), *Journal of Physics: Conference Series* 594 (2015) 012050.
11. K. Huang, *A Superfluid Universe*, World Scientific, 2016.
12. H. Hayasaka and S. Takenchi, *Phys. Rev. Lett.* **63**, 2701 (1989).
13. J. M. Nitschke and P.A Wilmarth, *Phys. Rev. Lett.* **64**, 2115 (1990).
14. J.E. Faller, W. J. Hollander, P.G. Nelson and M.P. McHugh, *Phys. Rev. Lett.* **64**, 825 (1990).
15. T.J. Quinn and A. Picard, *Nature (London)* **343**, 732(1990).
16. J. Luo, *Phys. Rev D*, **65**, 042005 (2002).
17. I. Lorincz and M. Tajmar, *Measurement* **73** (2015) pp. 453-461.
18. K. Thorne, *Plasma Physics*, Chapter 19, Section 19.4.3, pages 12-14, California Institute of Technology class notes Version 0619.1.K.pdf, March 28, 2007, Pasadena, CA.

High Frequency Gravitational Waves - Induced Propulsion

2017-01-2040

Published 09/19/2017

Salvatore Cezar Pais

Department of the Navy / NAVAIR

CITATION: Pais, S., "High Frequency Gravitational Waves - Induced Propulsion," SAE Technical Paper 2017-01-2040, 2017, doi:10.4271/2017-01-2040.

Abstract

It may be possible to generate high power / high frequency gravitational waves (HFGWs) by high frequency accelerated axial rotation (spin) and/or accelerated high frequency vibration of an electrically charged, possibly asymmetric structure, within the context of non-equilibrium thermodynamics, namely far-from-equilibrium physics, highly non-linear in nature.

The structure which is the HFGW generator (HFGWG), has the ability to control the accelerated modes of vibration and spin of its electrically charged surfaces, in particular the rapid rates of change of accelerated-decelerated-accelerated vibration and/or accelerated-decelerated-accelerated gyration (axial spin) of these electrified surfaces, in this manner delaying the onset of relaxation to thermodynamic equilibrium, thus generating a physical mechanism which may induce anomalous effects. Under certain conditions, involving rapid acceleration transients, it is observed that there will be exponential growth in electromagnetic energy flux with accelerating vibration. In the present paper, high power HFGWs are generated by enabling the Gertsenshtein effect, that is gravitational wave production by propagating electromagnetic radiation through strong magnetic fields.

Controlled motion of charged matter under rapid acceleration transients may enable macroscopic quantum coherence, namely possible quantum mechanical behavior of macroscopic objects. Moreover, the accelerated vibration and/or spin of charged matter may generate high power / high frequency gravitational waves which can be used in a variety of applications, such as advanced field propulsion, namely the design of a workable space drive.

Therefore, it may be feasible to propel a hybrid craft equipped with an HFGWG, by producing high frequency gravitational waves which in turn generate their own gravitational fields upon which the craft would propagate in a 'wave-surfing' fashion.

Introduction

On February 11, 2016 the National Science Foundation publicly announced that the Laser Interferometer Gravitational Wave Observatory (LIGO) had finally detected gravitational waves from the collision of two stellar mass black holes, thereby showing the reality of such waves and further strengthening General Relativity (GR) theory predictions [1].

Think of gravitational waves as undulations in the structure of spacetime, or to be more exact "ripples" in the curvature of the spacetime fabric. They are propagating fluctuations in gravitational fields [2], which arise due to dynamics of massive physical entities, although the source of gravitational waves may not be massive in nature as long as its motion is represented by high frequency/high energy, far from equilibrium dynamics. This fact can be observed from the stress-energy-momentum tensor expression in the GR field equations.

It is important to note that because of their physical nature (the graviton being a spin 2 particle) these waves have the capability to penetrate solid matter at high frequency (HF), moving at the speed of light. Furthermore, similar to electromagnetic waves these gravitational waves (GWs) are carriers of energy and momentum. Moreover, GWs are transverse and quadrupolar in nature (stretching and squeezing space along their propagation path), and can be produced by accelerating asymmetric masses, which denotes the far from equilibrium phenomena, their emission represents.

Electromagnetic (EM) radiation, caused by accelerating electrically charged objects, when passed through a static magnetic field (of constant magnetic flux density) gives rise to gravitational waves at the same frequency with the EM radiation. This phenomenon is known as the Gertsenshtein Effect [3].

In the language of quantum field theory, the Gertsenshtein effect can be described as the mixing of a propagating photon with a graviton, via a Yukawa-type coupling mediated by a virtual photon from the background field.

The generation of high power high frequency gravitational waves (HFGWs) is just one application of the fundamental innovative principle behind this work, namely the enablement of macroscopic quantum coherence induced by controlled motion of charged matter, subjected to rapid acceleration transients. This principle can give rise to Emergent Physical Phenomena, such as, but not limited, to Superconductivity.

Artificially generated, high energy, electromagnetic fields can interact strongly with the local Vacuum energy state, an aggregate/collective state comprised of the superposition of all fluctuations in the collective of quantum fields (including EM and gravitational fields, among others) permeating a given spacetime locality [4]. According to quantum field theory, this strong interaction between the fields is based on the mechanism of transfer of vibrational energy between the fields, further inducing local fluctuations in adjacent quantum fields which permeate that spacetime locality (these fields may or may not be electromagnetic in nature).

Think of the local Vacuum energy state as the collective energy state (structure) comprised of the ground state of minimum energy (baseline fluctuations) that is the quantum vacuum, and the excited state of energy (induced fluctuations) generated by matter or any other source of energy in that spacetime locality [5]. According to quantum field theory, matter, energy, spacetime are emergent constructs which arise out of a foundational structure, the fundamental framework which is the Vacuum energy state. Matter is confined energy, bound within fields, and may be thought of as a spectrum of different vibrational (and possibly gyration) frequencies of the Vacuum energy state. The engineering of the Vacuum metastructure (since there are multiple Vacuum structures) has been discussed from a General Relativity perspective [6], and from a quantum field theory perspective [7].

Consider that we are immersed in an ocean of energy, the Vacuum energy state, yet ordinarily we seem not to interact with it. This is because under normal circumstances (at or near equilibrium regime), the Vacuum state is homogeneous, isotropic, Lorentz invariant, in other words it is symmetric. Break this symmetry (far-from-equilibrium regime), and strong interactions with the Vacuum energy state become possible, thus affecting the manner in which the collective fields exchange energy with one another.

If we perform a “gedankenexperiment” we observe that the coupling of high frequency spin with high frequency vibration (especially for rapidly accelerated spin/vibration) of an electrically charged system (object) puts every point on the boundary of the object in a state of coherent superposition, thereby inducing a macroscopic quantum phenomenon [8].

Furthermore, as observed from the Casimir effect, the boundary conditions of a physical system affect the local Vacuum energy state (VES) of that system (comprised of zero point EM energy (QED) among other types of field energies (QCD, Higgs, etc.)) thereby affecting the system’s physical properties. Thus by manipulating/modifying the boundary conditions of a physical system with respect to its local VES, we can alter the system’s physical properties.

With this in mind, in a recent paper [9], the author discusses the possibility of inertial (or gravitational) mass reduction using high energy electromagnetic (EM) fields, whereby high frequency accelerated vibration and /or high frequency accelerated spin of electrically charged systems (minimally charged, if so desired) can lead to local vacuum state polarization (EM energy flux values in excess of 10^{33} W/m² are feasible, with corresponding energy densities in excess of 10^{25} J/m³), in this manner modifying the local spacetime lattice energy density. These systems would be strategically placed on an intergalactic craft.

The craft mass reduction effects are achieved by control, namely coherence, of the collective quantum fluctuations in the Vacuum energy state in the immediate vicinity of the aerospace vehicle/spacecraft’s electrified outer mold skin. As a result, extreme craft speeds can be achieved.

In a nutshell, this concept relates to an EM device which induces vibratory mass / energy fluctuations within a structure, which may or may not be solid in nature, thus generated EM plasma non-linearities may be considered.

An important realization (mathematically shown) of this aforementioned work is the fact that in an accelerated vibration and/or accelerated spin mode, the system’s EM energy flux is amplified by a factor equivalent to the product of vibrational (or spin) angular frequency and the operational time of acceleration (namely the time for which system is operated at maximum acceleration), with respect to the non-accelerated system’s EM energy flux (showing the importance of an accelerated departure far from thermodynamic equilibrium).

It is very important that the craft has the ability to control the accelerated modes of vibration and spin of the electrically charged surfaces, in particular the rapid rates of change of accelerated-decelerated-accelerated vibration and/or accelerated-decelerated-accelerated gyration (axial spin) of the electrified surfaces.

In this manner we can delay the onset of relaxation to thermodynamic equilibrium, thereby delaying maximal entropy production, thus generating a physical mechanism which may induce anomalous effects. In this case, the system’s EM energy flux is amplified by a factor equivalent to the square of the product of vibrational (or spin) angular frequency and the operational time of acceleration (time while system is at maximum acceleration), with respect to the non-accelerated system’s EM energy flux.

Going back to our subject matter at hand, a report written by the JASON group of the MITRE Corporation [10] for the Office of the Director of National Intelligence (Defense Intelligence Agency) comes to the conclusion that current means and methods of producing HFGW do not constitute a national security threat and in no shape or form can such physical entities be used for advanced propulsion or communication of any type.

The JASON report considers relatively low EM energy fluxes, when compared with those generated by the physical mechanisms described in reference 2 (on the order of 10^{33} W/m², and beyond). This exceptionally high EM power intensity induces spontaneous particle pair production (avalanche), thereby ensuring complete

polarization of the local Vacuum energy state, thus resulting in modification of the local spacetime energy density. It is this possibility which may alter the aforementioned report's conclusions.

Novel Propulsion Concept

As originally observed in reference 2, for conditions of accelerated vibration or accelerated spin of an electrically charged object/system, we can write for the maximum EM energy flux (time rate of change of EM energy transfer per unit surface area):

$$S_{\max} = f_G (\sigma^2 / \epsilon_0) [(R_v v^2) t_{\text{op}}] \quad (1)$$

, where f_G is the charged system geometric shape factor (equal to 1 for a disc configuration), σ is the surface charge density, ϵ_0 is the electrical permittivity of free space, R_v is the vibration (harmonic oscillation) amplitude, v is the angular frequency of vibration in Hertz, and similarly in the case of axial spin R_v is the effective system radius, while v represents the angular frequency of rotation, and t_{op} is the operational time for which the electrically charged system is operated at maximum acceleration ($R_v v^2$). This closed form formulation is the result of the synthesis of classical electromagnetic field theory with the physics of simple harmonic motion.

Furthermore, for the case of rapid time rates of change of accelerated vibration / spin (rapid acceleration transients) of the charged system, given that the time differential of acceleration is non-zero, we obtain:

$$S_{\max} = f_G (\sigma^2 / \epsilon_0) [(R_v v^3) t_{\text{op}}^2] \quad (2)$$

This is a thought provoking formulation because it shows that even with moderate vibrational / spin frequencies in a rapidly accelerating mode, the EM energy flux is greatly amplified.

Thus if the product of all the controllable parameters in [equation 2](#) (other than the angular frequency of vibration) was of unit order, we can achieve energy flux values on the order of 10^{33} W/m² (endemic of the polarized Vacuum energy state) with low end microwave frequencies on the order of 10^7 Hz (inducing vibrations of a resonant cavity wall of equal or higher frequencies, depending on cavity material). This in itself may qualify as an interesting observation, showing the extensive capabilities of a high energy / high frequency electromagnetic field generator.

Furthermore if we consider adding to the equation representing simple harmonic motion an "energy/momentum-pumping" (negative damping) term (bv), endemic of system acceleration, where b is a constant and v is (dx/dt) , namely the speed of a vibrating mass (m), something interesting occurs, in that it can be shown that the maximum of the total energy (E_T) of the vibrating system can be written as:

$$E_T \approx m R_v^2 \Omega^2 [\exp (2 \Omega t)] \quad (3)$$

, where Ω is the angular frequency of vibration, under the condition $[(\Omega = b/2m) \gg \Omega_0 \text{ (natural frequency of vibration)}]$. Since the EM energy flux is directly proportional to E_T , we observe that there will be exponential growth in energy flux with accelerating vibration, especially under the condition of rapid acceleration transients. Considering a classical Newtonian second law expression using the Lorentz (EM) force, we can relate the vibrating mass (m) with its vibrating charge (Q), in that m becomes directly proportional to the square of the ratio (Q / Ω). Coupling this relation with [equation 3](#) yields:

$$S_{\max} \approx (Q^2 / \epsilon_0) (R_v^2 / R_s^5) \Omega [\exp (2 \Omega t)] \quad (4)$$

[Equation 4](#) represents the maximum EM flux that can be achieved by accelerated vibration under the aforementioned condition, and applies to a spherical geometry (radius R_s) for a vibrating mass (m) of corresponding charge (Q).

Referring to the JASON report [10] we note that enabling the Gertsenshtein effect will result in the generation of a gravitational wave (out) by passing an electromagnetic wave (in) through a strong static magnetic field (these waves are of equal frequency). By combining equations 3-13 and 3-14 on page 10 of the report we obtain [equation 5](#):

$$P_{\text{GW(out)}} = [(4\pi G / c^4) B_0^2 L^2] P_{\text{EM(in)}} \quad (5)$$

, where G is the universal gravitational constant, c is the speed of light in free space, B_0 is the magnetic flux density of the static magnetic field operating over a distance L , and $P_{\text{GW(out)}}$ is the gravitational wave power achieved from an electromagnetic wave of power $P_{\text{EM(in)}}$.

It is important to note that a simple dimensional analysis shows that there is a factor missing in [equation 5](#) (as written in the JASON Report) equal to the inverse of the magnetic permeability of free space, namely a factor on the order of 10^6 .

Omitting this fact however, we can still show that by using a high frequency / high energy electromagnetic field generator we can produce HFGW exhibiting power levels on the order of 10^{10} watts, for an input EM energy flux on the order of 10^{33} W/m², where B_0 is the magnetic flux density, on the order of 10^{10} Tesla which is also produced with accelerated motion of charged matter under rapid acceleration transients.

Furthermore, by using equation 3-25 in reference 10, we can show that such HFGW power levels are equivalent to 10^{35} gravitons/sec production rates.

These extremely high graviton production rates further show that if multiple high power, high frequency gravitational waves were to be focused on a particular point in a spacetime locality, they can induce a spacetime curvature singularity, namely a "highly distorted and disrupted patch of spacetime fabric" [11].

We can conceive of a spinning and or vibrating asymmetric quadra-polar configuration of a plurality of EM resonant cavities in which specially arranged microwave emitters produce the accelerated vibrations necessary to generate the HFGWs, via the Gertsenshtein effect.

From a propulsion perspective, a craft equipped with a plurality of HFGW generators (HFGWG) induces curvature singularities in its close proximity, generating a gravitational well in its flight path, thereby “rolling down” this spacetime curvature dip, in a manner analogous to surfing.

Enablement of Propulsion Concept

The coupling of high spin frequency with high vibration frequency in order to achieve gravitational field manipulation/modification via the Gertsenshtein effect will enable the design of a hybrid craft, as shown in [figure 1](#). This hybrid aerospace/underwater craft (HAUC) configuration utilizes microwave-induced vibration within a resonant annular cavity, which features electrically charged outer mold line skin. The manner and effectiveness with which the microwave energy couples with the resonant cavity inner wall is called the cavity Q-factor. This parameter can be written as the (Energy stored / Energy lost) ratio and is in the range of 10^4 to 10^9 (and beyond), depending on whether ordinary metal (Aluminum or Copper at room temperature) or cryogenically cooled superconducting material (Yttrium Barium Copper Oxide or Niobium) is used for the resonant cavity inner wall and outside mold line skin of the aerospace vehicle.

The electrified skin of the craft can be further vibrated in an accelerated manner using imbedded lead zirconate titanate (PZT) modules (details not shown in [figure 1](#) due to possible security classification) which would generate the strong magnetic fields necessary for the enablement of the Gertsenshtein effect (nested EM fields). If the HAUC craft has a modular electrified outer skin design, composed of an ensemble/collective of miniaturized electrically charged surfaces, independently or collectively vibrated, then the craft can be very large in size.

Consequently, the generated high energy / high frequency electromagnetic flux would induce repulsive EM energy fields while in earth's atmosphere, thereby repelling air and water molecules in the craft's flight path.

Once in orbital space, HFGW-induced gravitational field manipulation would permit swift movement of the hybrid craft, which comes in conical or lenticular triangle /delta wing configurations, beyond our Solar System. A plurality of microwave antennas (high radio frequency emitter sources) in the electromagnetic spectrum range of 300 Megahertz to 300 Gigahertz are arranged within the annular duct - resonant cavity (surrounding the crew compartment and power plant system, which would be guarded in a Faraday-type cage, against all EM radiation effects), as portrayed in [figure 1](#).

An auxiliary conventional power plant/propulsion unit (not shown), would provide the initial hybrid vehicle thrust and electrical power generation. Furthermore, if the annular resonant cavity duct is filled with a noble gas such as Xenon, the microwave energy collision with the gas particles will induce a plasma state of matter (further

augmenting the oscillatory vibrations experienced by the resonant cavity inner wall), thereby creating a highly non-linear environment (phase transitions / abrupt changes of state from gas to plasma, which induce Symmetry-breaking) which will intensify non-linear effects, thereby augmenting induced HFGW power. This will intensify the coherence of quantum vacuum fluctuations in the proximity of the outside mold line skin (electrically charged) of the aerospace vehicle, in this manner assuring a high degree of Vacuum polarization.

Therefore it may be possible to envision a hybrid craft which due to the physical mechanisms enabled with HFGW generators (HFGWG) can function as a submersible craft capable of extreme underwater speeds (lack of water-skin friction) and enhanced stealth capabilities (non-linear scattering of RF and sonar signals). This hybrid craft would move with great ease through the air - space - water mediums, by being enclosed in a Vacuum plasma shield, due to the coupled effects of EM field-induced air/water particles repulsion and local Vacuum energy state polarization.

Potential HFGWG Applications

The implications of colliding/focusing HFGWs generated by rapidly accelerated vibration/spin of electrically charged systems can be used in applications of advanced field propulsion as well as the extreme disruption of a planetary body (if so desired) since it can be shown that the energy level (gain in potential energy) capable of annihilating a planet such as the Earth is on the order of 10^{32} Joules (possibly achieved with the concept at hand, considering $E_{\text{annihil}} = (3/5) (GM_p^2 / R_p)$; where E_{annihil} is the gravitational binding energy, the other variables being defined by Newton's law of universal gravitation). Imagine a plurality of HFGWG devices (a minimum of four modules), aligned around the planetoid along a planar axis (at the four cardinal points).

The emitted HFGWs would impinge on each other in such a manner as to severely disrupt the vacuum energy state at a spacetime locality denoting a point of impact (collision of gravitons with gravitons). At this disruption point, energy may be amplified to such a high degree as to generate a spacetime curvature singularity, leading to total destruction of the planetoid (asteroid).

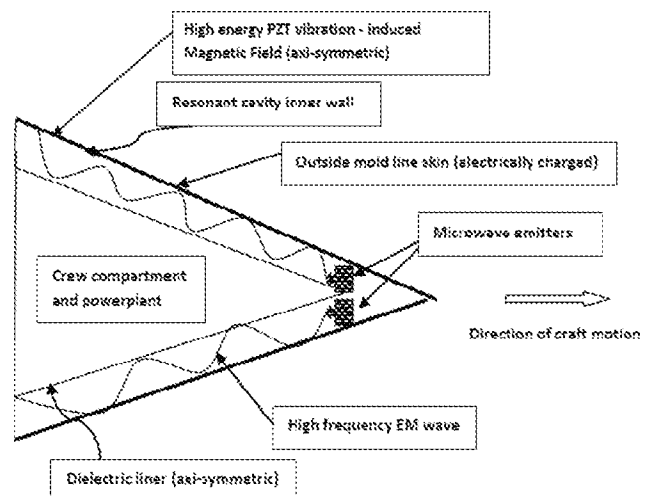


Figure 1. HFGWG - equipped craft configuration (cross-sectional view)

Moreover, considering that gravitons are spin 2 particles, hence they will not couple with the fermions / electrons (spin 1/2) of solid 'ordinary' matter (thus passing right through), we can devise new methods of communication through solid objects, as discussed in reference 11.

Nuclear fusion may also be engineered using the concept at hand, given the extremely high plasma densities and temperatures, as well as the high energy confinement times which can be achieved with the generation of ultra-high electromagnetic field intensities.

Conclusions

Perhaps, there is a simpler way of explaining the utilization of the HFGWG device as a propulsion unit; if we consider that this device is capable of concentrating a vast amount of energy in a relatively small space, thus locally de-stiffening / ripping / tearing the spacetime structure, thus permitting motion through the "void" within the vacuum.

As long as the device is on (and operated at high levels of accelerated vibration/spin), the HFGWG-equipped craft is capable of extreme speeds.

In parallel, if we think of the Universe as a superfluid, we may be able to say that the HFGWG device has the capability of inducing a local phase transition from a turbulent regime to a laminar regime, thus allowing for "smooth sailing" of a hybrid craft through the specially conditioned vacuum of Space (a vacuum that has undergone macroscopic quantum coherence, locally, around the craft). As a result, the craft experiences "suction" into the conditioned vacuum.

As an afterthought in regard to macroscopic quantum coherence, the controlled motion of charged matter under rapid acceleration transients may lead to room temperature superconductivity. There are three parameters which control superconductivity, namely temperature, current density and externally applied magnetic field strength. These three parameters have one thing in common, namely the motion of electric charges (electrons).

Since this motion can be strongly controlled by accelerated vibration and/or accelerated spin of charged matter (possibly inhomogeneous) under condition of rapid acceleration transients, it may possibly lead to room temperature superconductivity.

References

1. Abbott B.P. et al., Observation of gravitational waves from a binary black hole merger, PRL, 116, 061 102 (2016).

2. Kokkotas K.D., Gravitational wave physics, Encyclopedia of Physical science and Technology, 3rd Edition, Volume 7, Academic Press, 2002.
3. Gertsenshtein M.E., Wave resonance of light and gravitational waves, J. Exptl. Theoret. Phys. (USSR) 41, 113-114 (1961).
4. Millis M. and Davis E., Frontiers of propulsion science, AIAA Progress in Astronautics and Aeronautics, Vol. 227, pp 199-201, 404, 2008.
5. Rafelski J. and Muller B., The structured vacuum, Verlag Harri Deutsch, 1985.
6. Putthoff H.E., Advanced space propulsion based on vacuum (spacetime metric) engineering, JBIS, Vol. 63, pp 82-89, 2010.
7. Froning H.D., Quantum vacuum engineering for power and propulsion from the energetics of space, presented at the Third International Conference on future Energy, Washington D.C. October 9-10, 2009.
8. O'Connell A.D. et al., Quantum ground state and single-phonon control of a mechanical resonator, Nature 464, 697-703, April 1, 2010.
9. Pais S.C., The high energy electromagnetic field generator, Int. J. Space Science and Engineering, Vol.3, No. 4, 2015 pp.312-317.
10. Pandolfi R., High frequency gravitational waves, The MITRE Corporation, JASON Program Office, prepared for The Office of the Director of National Intelligence, DIA, report number JSR-08-506, October 2008.
11. Fontana G., Gravitational wave propulsion, Proceedings of Space Technologies and Applications International forum, STAIF 2005.

Contact Information

Dr. Salvatore Cezar Pais, Ph.D.
Department of the Navy, NAVAIR / NAWCAD, NAS Patuxent River
Maryland 20670
salvatore.pais@navy.mil
scpdraconis@yahoo.com

Acknowledgments

Funding for this work was provided by the Naval Innovative Science & Engineering (NISE) - Basic & Applied Research (BAR) program, under the project name "The High Energy Electromagnetic Field Generator (HEEMFG)", project number 219BAR-17-009. I wish to thank Dr. James Sheehy, Chief Technology Officer, Naval Aviation Enterprise, for the numerous enlightening discussions on this innovative concept.

The Engineering Meetings Board has approved this paper for publication. It has successfully completed SAE's peer review process under the supervision of the session organizer. This process requires a minimum of three (3) reviews by industry experts.

This is a work of a Government and is not subject to copyright protection. Foreign copyrights may apply. The Government under which this paper was written assumes no liability or responsibility for the contents of this paper or the use of this paper, nor is it endorsing any manufacturers, products, or services cited herein and any trade name that may appear in the paper has been included only because it is essential to the contents of the paper.

Positions and opinions advanced in this paper are those of the author(s) and not necessarily those of SAE International. The author is solely responsible for the content of the paper.

ISSN 0148-7191

<http://papers.sae.org/2017-01-2040>

Estimation of Q -Factors and Resonant Frequencies

Kevin J. Coakley, Jolene D. Splett, Michael D. Janezic, *Senior Member, IEEE*, and Raian F. Kaiser

Abstract—We estimate the quality factor Q and resonant frequency f_0 of a microwave cavity based on observations of a resonance curve on an equally spaced frequency grid. The observed resonance curve is the squared magnitude of an observed complex scattering parameter. We characterize the variance of the additive noise in the observed resonance curve parametrically. Based on this noise characterization, we estimate Q and f_0 and other associated model parameters using the method of weighted least squares (WLS). Based on asymptotic statistical theory, we also estimate the one-sigma uncertainty of Q and f_0 . In a simulation study, the WLS method outperforms the 3-dB method and the Estin method. For the case of measured resonances, we show that the WLS method yields the most precise estimates for the resonant frequency and quality factor, especially for resonances that are undercoupled. Given that the resonance curve is sampled at a fixed number of equally spaced frequencies in the neighborhood of the resonant frequency, we determine the optimal frequency spacing in order to minimize the asymptotic standard deviation of the estimate of either Q or f_0 .

Index Terms—Cylindrical cavity, experimental design, microwave, noise characterization, optimal frequency spacing, quality factor, resonance curve, resonant frequency.

1. INTRODUCTION

IN THIS study, we characterize the frequency-dependent additive noise in measured microwave cavity resonance curves and estimate the quality factor Q and resonant frequency f_0 of the microwave cavity. The data used are the squared magnitudes of the observed values of frequency-dependent complex scattering parameters $|S_{21}|^2$.

The resonance curve parameters Q and f_0 can be estimated from the observed values of $|S_{21}|^2$ using either the 3-dB or the Estin method [1]. The Estin method is an example of a resonance curve area (RCA) method [2]. In these approaches, the estimated resonant frequency is the frequency at which the resonance curve reaches its maximum value. Hence, the estimated resonant frequency is constrained to take discrete values. Further, neither the 3-dB nor the Estin method exploits knowledge about frequency-dependent additive noise in the data. In related work, Petersan and Anlage [3] demonstrated that the method of least squares (LS) provides superior estimates of Q and f_0 when compared to the 3-dB method and to the related RCA method for a similar resonance curve problem. However, for cases where the variance of the additive noise varies with frequency, the method of LS is suboptimal. Further, the LS method

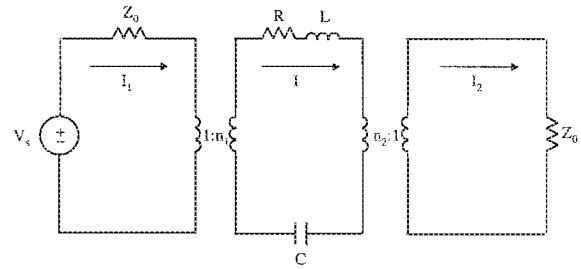


Fig. 1. Resonant cavity equivalent circuit model.

does not provide an estimate of the covariance of the estimated model parameters.

Here, we present a new method to estimate Q and f_0 that accounts for frequency-dependent additive noise. We characterize the frequency-dependent noise in the measured resonance curve in terms of a parametric model with two parameters. In the statistical literature, such an approach is known as variance function estimation [4]. In our model, one parameter corresponds to a noise floor, while the other parameter represents the frequency-dependent part of the noise. Based on the estimated variance function parameters, we estimate the resonance curve parameters (including Q and f_0) using the weighted least squares (WLS) method. Due to the sensitive nature of this optimization problem, we take special care to ensure that we find (or very nearly find) the global minimum of the objective function that we seek to minimize. In particular, instead of starting our optimization algorithm from just one set of initial guesses for the model parameters, we perform the optimization algorithm for each of many randomly selected initial guesses.

Based on the estimated variance function parameters and estimated resonance curve model parameters, we estimate the one-sigma random errors of Q and f_0 using asymptotic statistical theory. In our experiments, the resonance curve is sampled at 201 equally spaced frequencies in the neighborhood of the resonant frequency. We compute the asymptotic standard deviation of the Q and f_0 estimates as a function of the frequency spacing df , the model parameters that characterize the resonance curve, and the additive noise. For optimal estimation of Q , using our experimental data, $\Delta = Q(f_{\max}/f_0 - 1) \approx 2.6$, where f_{\max} is the largest frequency. For optimal estimation of f_0 , $\Delta \approx 0.6$.

II. RESONANCE CURVE MODEL

We model a two-port cylindrical cavity with the equivalent circuit shown in Fig. 1 [5], [6]. In particular, we are interested in measuring an undercoupled cavity, with a high quality factor, operating near resonance. In this case, we assume that the resistances and self-inductances of the coupling loops are negligible [5]. We employ two ideal transformers to model the coupling

Manuscript received April 1, 2002; revised September 23, 2002.

K. J. Coakley and J. D. Splett are with the Statistical Engineering Division, National Institute of Standards and Technology, Boulder, CO 80305 USA (e-mail: kevin.coakley@nist.gov; jolene.splett@nist.gov).

M. D. Janezic and R. F. Kaiser are with the RF Technology Division, National Institute of Standards and Technology, Boulder, CO 80305 USA (e-mail: michael.janezic@nist.gov; raian.kaiser@nist.gov).

Digital Object Identifier 10.1109/TMTT.2003.808578

loops that excite the cylindrical cavity. We use a series inductor (L), capacitor (C), and resistor (R) to model the cylindrical cavity. An impedance-matched source is connected to port one of the cavity while an impedance-matched load is connected to port two. Note that the source and load can be interchanged without loss of generality.

We define $T(f)$ as the transmission loss through the cylindrical cavity

$$T(f) = \frac{P_{\text{in}}}{P_L} \quad (1)$$

where f is the frequency, P_{in} is the maximum power delivered to a matched load connected at port one, and P_L is the maximum power delivered to the load at port two [5]. Solving for P_{in} and P_L we find

$$P_{\text{in}} = I_1 I_1^* Z_0 = \frac{V_s^2}{4Z_0} \quad (2)$$

and

$$P_L = I_2 I_2^* Z_0 = \frac{V_s^2}{Z_0} \frac{\beta_1 \beta_2}{(1 + \beta_1 + \beta_2)^2 + Q_0^2 \left(\frac{f}{f_0} - \frac{f_0}{f} \right)^2} \quad (3)$$

where

$$\beta_1 = \frac{n_1^2 Z_0}{R} \quad (4)$$

and

$$\beta_2 = \frac{n_2^2 Z_0}{R}. \quad (5)$$

In (3), the resonant frequency f_0 is defined as

$$f_0^2 = \frac{1}{4\pi^2 LC} \quad (6)$$

and the unloaded quality factor Q_0 is

$$Q_0 = \frac{2\pi f_0 L}{R}. \quad (7)$$

Substituting (2) and (3) into (1) we obtain

$$T(f) = \frac{4\beta_1 \beta_2}{(1 + \beta_1 + \beta_2)^2 + Q_0^2 \left(\frac{f}{f_0} - \frac{f_0}{f} \right)^2}. \quad (8)$$

At resonance ($f = f_0$), the transmission loss reduces to

$$T(f_0) = \frac{4\beta_1 \beta_2}{(1 + \beta_1 + \beta_2)^2}. \quad (9)$$

Taking the ratio of $T(f_0)/T(f)$ we obtain

$$\frac{T(f_0)}{T(f)} = 1 + \frac{Q_0^2 \left(\frac{f}{f_0} - \frac{f_0}{f} \right)^2}{(1 + \beta_1 + \beta_2)^2}. \quad (10)$$

Note that, in practice, the unloaded quality factor Q_0 is larger than the measured quality factor Q due to the effects of the coupling loops

$$Q_0 = Q(1 + \beta_1 + \beta_2). \quad (11)$$

However, if we reduce the coupling level so that the cylindrical cavity is very undercoupled ($\beta_1 \ll 1$ and $\beta_2 \ll 1$), we can neglect the coupling factors β_1 and β_2 and rewrite (10) as

$$T(f) = \frac{T(f_0)}{1 + Q^2 \left(\frac{f}{f_0} - \frac{f_0}{f} \right)^2} \approx \frac{T(f_0)}{1 + Q_0^2 \left(\frac{f}{f_0} - \frac{f_0}{f} \right)^2} \quad (12)$$

with the assumption that the measured quality factor Q is approximately Q_0 . (If coupling cannot be ignored, see [7] for methods of calculating β_1 and β_2 .)

At the k th frequency, we model the measured resonance curve as

$$T_m(f_k) = \frac{T(f_0)}{1 + Q^2 \left(\frac{f_k}{f_0} - \frac{f_0}{f_k} \right)^2} + \text{BG} + \epsilon(f_k) \quad (13)$$

where $T_m(f_k) = |S_{21}(f_k)|^2$ represents the observed measurement, $T(f_k)$ denotes the true value or “noise-free” measurement, BG is a noise floor, and $\epsilon(f_k)$ is additive noise with an expected value of zero and variance $\sigma_{\epsilon(f_k)}^2$. The model parameters form a four-vector, $\vec{\theta} = (\theta_1, \theta_2, \theta_3, \theta_4) = (T(f_0), Q, f_0, \text{BG})$. For the observed data, we model the variance of the additive noise as

$$\text{VAR}[\epsilon(f_k)] = \sigma_{\epsilon(f_k)}^2 = \frac{\gamma_1^2}{1 + Q^2 \left(\frac{f_k}{f_0} - \frac{f_0}{f_k} \right)^2} + \gamma_2^2 \quad (14)$$

where γ_1 and γ_2 correspond to the frequency-dependent noise and the noise floor, respectively. In Appendix C, we prove that our variance function model (14) is exact for the case where the additive noise in the measurement of the real part of S_{21} and the additive noise in the measurement of the imaginary part of S_{21} are statistically independent realizations of the same Gaussian process. In our proof, we assume that the expected values of the additive noise realizations are zero.

A. Parameter Estimation

Suppose we measure the resonance curve at M distinct frequencies and estimate the model parameters by minimizing a weighted sum of M squared residuals

$$L = \sum_{k=1}^M w_k [T_m(f_k) - \hat{T}_m(f_k)]^2. \quad (15)$$

If the weights w_k are all equal, minimization of L yields the LS estimate of $\vec{\theta}$. If the k th weight is set to the reciprocal of the (estimated) variance of $T_m(f_k)$, i.e., $w_k = 1/\text{VAR}[T_m(f_k)]$, then minimization of L yields the WLS estimate of $\vec{\theta}$.

We assume that additive noise realizations are statistically independent. Given the parameters which characterize the resonance curve $\vec{\theta}$ and the variance of the additive noise, asymptotic theory [8] predicts the covariance of the parameter estimates. From one curve, the predicted covariance is

$$\widehat{\text{COV}}(\hat{\vec{\theta}}) = (B^T V^{-1} B)^{-1} \quad (16)$$

where the elements of the diagonal matrix V are

$$V_{kk} = \text{VAR}[T_m(f_k)] \quad (17)$$

and

$$B_{kj} = \frac{\partial \langle T_m(f_k) \rangle}{\partial \theta_j}. \quad (18)$$

Thus, the predicted asymptotic variance of the m th parameter estimated from a resonance curve is

$$\sigma_{\theta_m}^{*2} = (B^T V^{-1} B)_{mm}^{-1}. \quad (19)$$

Alternatively, the asymptotic standard error (ASE) of the estimate of θ_m is

$$\sigma_{\theta_m}^* = \sqrt{(I^{-1})_{mm}} \quad (20)$$

where

$$I_{ij} = \sum_{k=1}^M \frac{1}{\text{VAR}[T_m(f_k)]} \frac{\partial \langle T_m(f_k) \rangle}{\partial \theta_i} \frac{\partial \langle T_m(f_k) \rangle}{\partial \theta_j}. \quad (21)$$

The ASE can be thought of as an approximation for the standard deviation of the parameter. As the signal-to-noise ratio (SNR) of the data increases, the accuracy of this approximation improves in general. For more discussion of asymptotic properties of estimates of nonlinear WLS, see [8].

B. Computational Details

The algorithm for estimation of Q and f_0 has four steps.

- Step 1) Compute \hat{Q} using the Estin method [1]. (See Appendix A.)
- Step 2) Use \hat{Q} from the Estin method as a starting value in the nonlinear fitting algorithm that computes unweighted LS estimates of the model parameters. The background parameter BG is constrained to be positive by expressing it as the squared value of the appropriate parameter in the model.
- Step 3) Estimate the variance function and weights based on the “binned” squared residuals by the method of LS. Frequency bins were determined by dividing the entire frequency range of the resonance curve into 40 equal sections. The variance estimates were adjusted upward by a degree of freedom factor of 201/197.

Although the variance is modeled using γ_1^2 and γ_2^2 to ensure a positive variance estimate, the optimization code searches for a solution in the unconstrained γ_1 and γ_2 space. We report $|\hat{\gamma}_1|$ and $|\hat{\gamma}_2|$.

A typical variance function is shown in Fig. 2(c). The vertical axis displays the fractional residuals, which are absolute residuals divided by $\hat{\theta}_1$, and the horizontal dashed line near the bottom of the plot represents the fractional background level, $\hat{\gamma}_2/\hat{\theta}_1$. Fig. 2(d) displays the same data when residuals are assigned to frequency bins and the average fractional residual is computed for each bin.

- Step 4) Use the *unweighted* LS parameter estimates as starting values in the nonlinear fitting algorithm that computes *weighted* LS parameter estimates. The weights used in the nonlinear fit are derived from the variance function estimated in step 3.

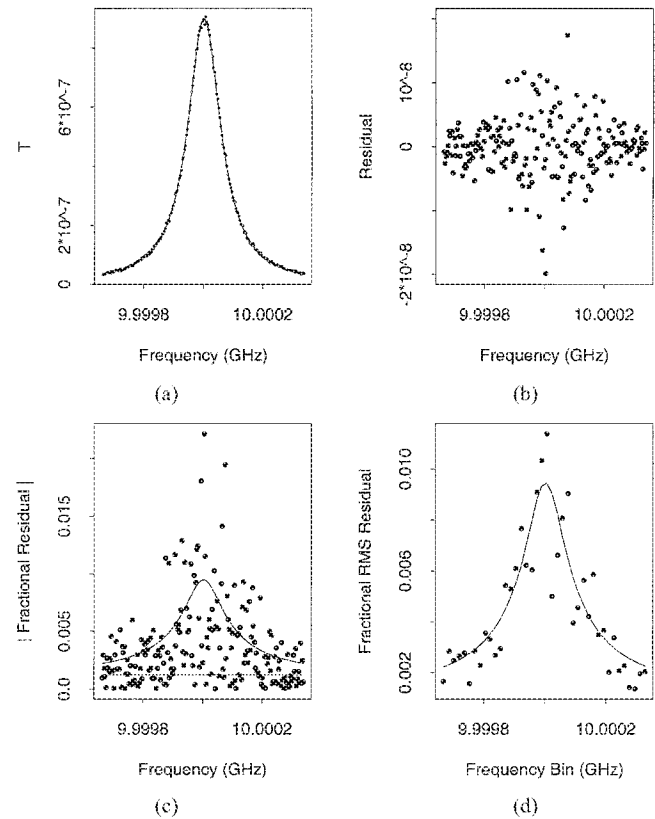


Fig. 2. (a) An observed and predicted (from WLS fit) resonance curve. (b) Raw residuals. (c) Fractional residuals (absolute residuals divided by $\hat{\theta}_1$). (d) Binned fractional rms residuals versus frequency. In (a) and (d), model predictions are shown as solid lines.

The nonlinear fitting routine used to determine the LS and WLS parameter estimates minimizes a general, unconstrained objective function using the analytic gradient and Hessian of the objective function [9].

The objective function was minimized for each of 250 randomly generated initial parameter values. The final parameter estimates are those that yield the smallest value of the objective function. If only one set of initial parameter values is used, the objective function may converge to a local minimum rather than the global minimum.

The same nonlinear fitting routine used to compute LS and WLS parameter estimates was also used to estimate the variance function parameters. Again, we experienced convergence problems, so random initial parameter values were used.

III. EXPERIMENTAL STUDY

In our study, we employed a cylindrical cavity resonator, shown in Fig. 3. The cavity was nominally 450 mm long and 60 mm in diameter, and it was composed of a helically wound cylindrical waveguide terminated by two endplates. Both of the gold-plated endplates were optically polished. One endplate was fixed on the top of the cylindrical cavity, while the bottom endplate, with a slightly smaller diameter than that of the cylindrical waveguide, traveled over a range of 25 mm through the use of a motorized micrometer drive. Movement of the bottom endplate allowed for tuning of the cavity resonant frequency.

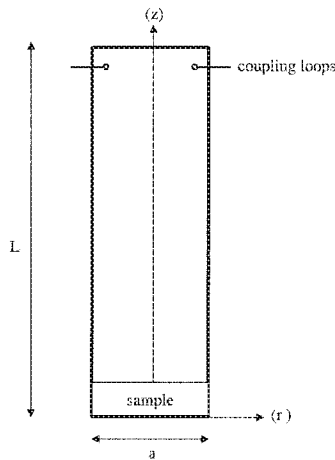


Fig. 3. Cylindrical cavity in the “sample loaded” state.

As in [10] and [11], use of a helical waveguide attenuated many of the undesired resonant modes while allowing the TE_{01n} cavity modes to propagate. Our particular helical waveguide consisted of two copper wires embedded in epoxy surrounded by a fiberglass cylinder. Although the helical waveguide lowered the quality factor of the cavity slightly, it also eliminated many of the unwanted resonant modes. Thus, the advantages of using the helical waveguide outweighed its associated disadvantages.

Near the top of the cylindrical waveguide section were two coupling loops, extending from two coupling holes located on opposite sides of the cylindrical waveguide. In order to excite a resonance in the cylindrical cavity, each coupling loop was connected to an automatic network analyzer via a coaxial transmission line. Cavity coupling was altered by changing the extent that the coupling loops protruded into the cavity. In particular, we kept the resonant peak amplitude below -50 dB so that the losses due to the coupling loops were negligible.

We operated the cylindrical cavity in two states, “air” and “sample loaded.” The “air” state refers to the cavity without a sample present, while the “sample loaded” state refers to the cavity with a dielectric sample on the bottom endplate. We adjusted the cylindrical cavity length to obtain a resonant frequency near 10 GHz for each cavity state. For each cavity state, 30 resonance curves were collected at two different frequency spacings df . Each resonance curve was made up of 201 equally spaced points, and we performed 512 averages on each resonance curve to reduce the level of noise. For each curve, we estimated \hat{Q} and \hat{f}_0 by various methods. Fig. 4 displays the estimates of Q and f_0 for each of the 30 experimental curves corresponding to the “sample loaded” state. The binned fractional root-mean-square (rms) residuals and the estimated variance functions are shown in Fig. 5 for the 30 “sample loaded” resonance curves.

Tables I and II display mean estimates of Q and f_0 and their associated standard deviations (shown in parentheses) for the various methods. For each curve, we estimated the ASE based on the parameter estimates and (20). The WLS method yields estimates with the lowest variability.

For 30 realized data sets, a 95% two-sided confidence interval for σ is $(0.7964\hat{\sigma}, 1.3443\hat{\sigma})$. Thus, the sampling error is not

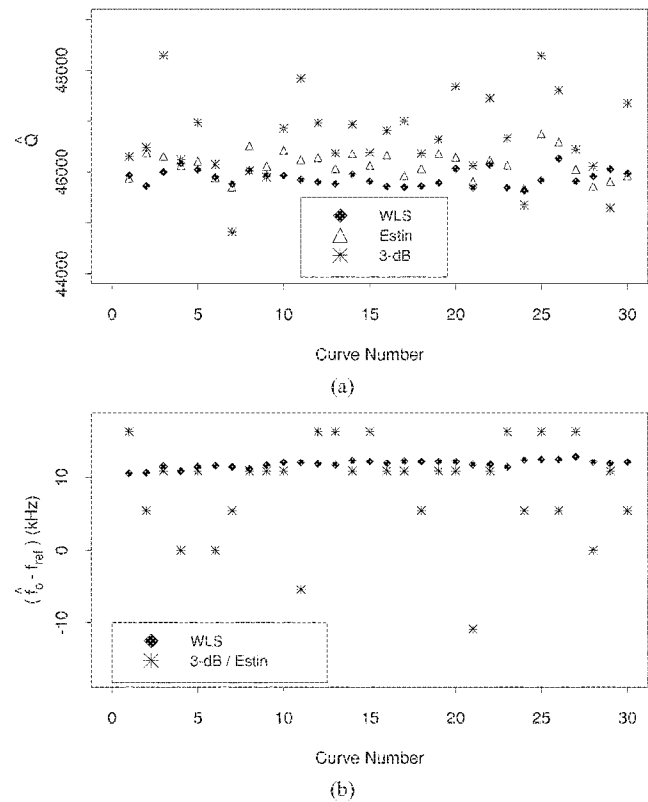
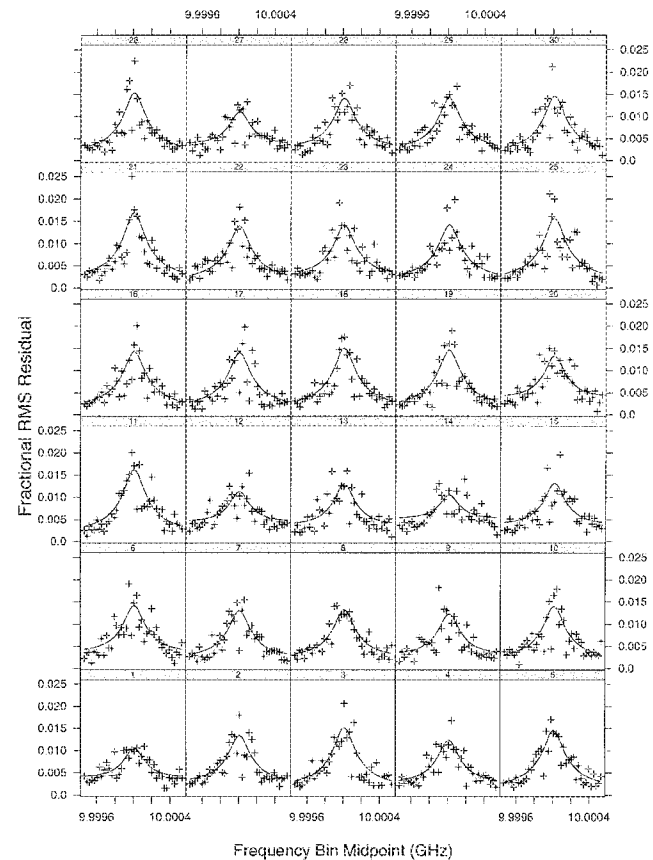
Fig. 4. Estimated values of: (a) Q and (b) $f_0 - f_{ref}$ ($f_{ref} = 10$ GHz) for each of 30 experimental curves corresponding to the “sample loaded” state where $\Delta = 2.4396$.

Fig. 5. Predicted (lines) and observed variance functions for 30 observed resonance curves corresponding to the “sample loaded” state.

TABLE I

STATISTICAL PROPERTIES OF Q ESTIMATES COMPUTED FROM REAL DATA INCLUDING: THE MEAN OF \hat{Q} , STANDARD ERROR OF THE MEAN (SHOWN IN PARENTHESES), AND THE STANDARD ERROR OF \hat{Q} . FOR THE WLS METHOD, WE LIST THE MEAN ESTIMATE OF $\sigma_{\hat{Q}}^*$, THE ASE OF \hat{Q} (20), AND ITS ASSOCIATED STANDARD ERROR

Cavity State	df (Hz)	Estim	3-dB	LS	WLS	$\sigma_{\hat{Q}}^*$
air	3400	74335(45)	75051(140)	74119(61)	74081(44)	
		246	766	334	241	238(3)
	1000	75150(90)	75406(117)	74143(63)	74153(55)	
sample loaded	5400	46143(49)	46659(150)	45885(40)	45888(29)	
		270	823	218	161	206(3)
	1500	47225(70)	47303(110)	46029(53)	46020(48)	
		381	605	292	263	483(5)

TABLE II

STATISTICAL PROPERTIES OF f_0 ESTIMATES COMPUTED FROM REAL DATA INCLUDING: THE MEAN OF $\hat{f}_0 - f_{ref}$ ($f_{ref} = 10$ GHz), STANDARD ERROR OF THE MEAN (SHOWN IN PARENTHESES), AND THE STANDARD ERROR OF \hat{f}_0 . FOR THE WLS METHOD, WE LIST THE MEAN ESTIMATE OF $\sigma_{\hat{f}_0}^*$, THE ASE OF \hat{f}_0 (20), AND ITS ASSOCIATED STANDARD ERROR

Cavity State	df (Hz)	Estim	3-dB	LS	WLS	$\sigma_{\hat{f}_0}^*$
air	3400	$\hat{f}_0 - f_{ref}$ (Hz)	2365(651)	1424(81)	1458(79)	
			3565	444	435	125(2)
	1000	-2381(653)	-3249(119)	-3245(119)		
sample loaded	5400	8696(1239)	11534(94)	11845(98)		
		6785	517	537	280(5)	
	1500	8530(960)	9710(45)	9751(44)		
		5258	249	239	182(2)	

large enough to explain the discrepancy between the empirical standard deviation of the Q estimates and the estimated ASE at $df = 1000$ Hz and 1500 Hz.

The asymptotic standard error of \hat{f}_0 is much smaller than the estimated standard deviation of \hat{f}_0 computed from the 30 resonance curves. We attribute this discrepancy to systematic drift of the resonant frequency during the experiment. The variability of the Estim/3-dB estimate is much larger than the variability of the LS and WLS estimates.

IV. THEORETICAL STUDIES

A. Optimal Frequency Spacing

Based on $\bar{\theta}$ and $\bar{\gamma}$, we compute asymptotic standard errors $\sigma_{\hat{Q}}^*$ and $\sigma_{\hat{f}_0}^*$ using (14)–(21). In our first study, we equate the resonance frequency to the model parameters of the corresponding mean values computed from the observed resonance curves (Table III). In all cases, the resonance curve is sampled at 201 equally spaced frequencies. We define

$$\Delta = Q \frac{f_{\max} - f_0}{f_0} \quad (22)$$

where $f_{\max} = f_0 + 100df$. In Fig. 6, we show the fractional asymptotic standard error (ASE) of the estimates of Q and f_0 as a function of df . The optimal values of df for estimation of Q and f_0 are listed in Table IV.

TABLE III

PARAMETER VALUES USED IN THE SIMULATION $f_{ref} = 10$ GHz

Parameter	"sample loaded" $df = 5400$ Hz	"air" $df = 3400$ Hz
$\theta_1 \times 10^6$	446.4	894.3
θ_2	45888	74081
$\theta_3 - f_{ref}$ (Hz)	11845	1458
$\theta_4 \times 10^9$	0.20	0.28
$\gamma_1 \times 10^9$	6.37	8.80
$\gamma_2 \times 10^9$	0.95	1.21

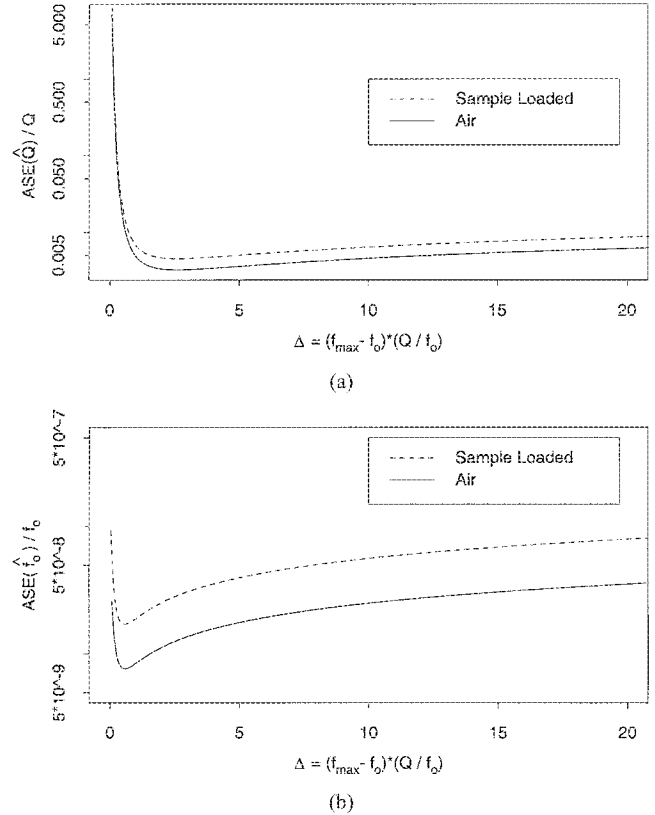


Fig. 6. Fractional asymptotic standard errors of: (a) \hat{Q} and (b) \hat{f}_0 where model parameters are equated to estimated values from real data. Values of Q are 74 081.32 and 45 888.34 for "air" and "sample loaded" cavity states, respectively.

TABLE IV
THEORETICAL ASEs (20) OF \hat{Q} AND \hat{f}_0 BASED ON DATA SIMULATED USING TABLE III PARAMETER VALUES

Parameter Estimate	Cavity State	df (Hz)	Δ	Theoretical ASE
\hat{Q}	air	1000	0.7482	516.181
		3400	2.5262	240.030
		3500 ^a	2.6003	239.940
	sample loaded	1500	0.6929	501.346
		5400	2.4826	208.045
\hat{f}_0	air	5700 ^a	2.5743	207.924
	sample loaded	1500	0.6929	173.6 Hz
		5400	2.4826	281.1 Hz
		1400 ^a	0.6011	171.7 Hz

^a optimal

TABLE V

STATISTICAL PROPERTIES OF ESTIMATES OF Q COMPUTED FROM SIMULATION DATA INCLUDING: BIAS OF THE ESTIMATE, STANDARD ERROR OF THE BIAS (SHOWN IN PARENTHESES), AND THE STANDARD ERROR OF THE ESTIMATE. THE MEAN OF THE ESTIMATED VALUE OF ASE, ASE, IS SHOWN FOR THE WLS METHOD

Q	Spacing (Hz)	3-dB	Estin	WLS	ASE	ASE
74081	1000	1381(22)	1175(15)	176(10)		
	($\Delta = 0.7408$)	701	475	332	523	517
	3400	706(25)	183(11)	32(7)		
	($\Delta = 2.5188$)	804	339	209	234	235
	6800	279(26)	-215(18)	12(8)		
45888	($\Delta = 5.0375$)	831	562	253	250	259
	1500	1385(18)	1169(13)	173(10)		
	($\Delta = 0.6883$)	581	421	314	505	499
	5400	672(21)	220(9)	28(6)		
	($\Delta = 2.4780$)	652	286	179	202	203
	10800	344(22)	42(16)	12(7)		
	($\Delta = 4.9559$)	693	508	218	215	223

TABLE VI

STATISTICAL PROPERTIES OF f_0 ESTIMATES COMPUTED FROM SIMULATION DATA INCLUDING: BIAS OF THE ESTIMATE, STANDARD ERROR OF THE BIAS (SHOWN IN PARENTHESES), AND THE STANDARD ERROR OF THE ESTIMATE. THE MEAN OF THE ESTIMATED VALUE OF ASE, ASE, IS SHOWN FOR THE WLS METHOD

Q	Spacing (Hz)	3-dB/Estin (Hz)	WLS (Hz)	ASE (Hz)	ASE (Hz)
74081	1000	-156(104)	2(2)		
	($\Delta = 0.7408$)	3300	75	78	77
	3400	-17(12)	5(4)		
	($\Delta = 2.5188$)	3808	124	122	124
	6800	7(1324)	4(6)		
45888	($\Delta = 5.0375$)	4188	178	166	175
	1500	-368(193)	3(5)		
	($\Delta = 0.6883$)	6114	166	173	171
	5400	54(223)	11(9)		
	($\Delta = 2.4780$)	7044	275	271	276
	10800	130(242)	10(13)		
	($\Delta = 4.9559$)	7655	395	371	389

B. Monte Carlo Study

We simulate data similar to observed data for both cavity states. In Tables V and VI, we compare the performance of the various methods for estimating Q and f_0 . In Table VII, we list the statistical properties of our variance function parameter estimates. For the lowest frequency spacing, the standard errors of the Q estimates are lower than what is predicted by asymptotic theory. For the other frequency spacings, the asymptotic theory predicts the standard error of the Q estimate well. For all frequencies, the standard error of the f_0 estimate is well predicted by asymptotic theory.

V. SUMMARY

The frequency-dependent additive noise in measured microwave cavity resonance was characterized. The observed data were the squared magnitude of a frequency-dependent complex scattering parameter $|S_{21}|^2$. Based on a parametric model for the additive noise of the observed resonance curve, Q and f_0 and other associated model parameters were estimated using the method of WLS. Asymptotic statistical theory was used to estimate the one-sigma uncertainty of Q and f_0 . We found that the WLS method outperformed the 3-dB method and the Estin

TABLE VII

TRUE VARIANCE FUNCTION PARAMETERS IN SIMULATION STUDY AND MEAN VALUES OF ESTIMATED VARIANCE FUNCTION PARAMETERS. STANDARD ERRORS ARE SHOWN IN PARENTHESES

Q	$\gamma_1 \times 10^9$	$\gamma_2 \times 10^9$	df (Hz)	$\tilde{\gamma}_1 \times 10^9$	$\tilde{\gamma}_2 \times 10^9$
74081	8.7797	1.2058	1000	8.15(4)	2.19(5)
			3400	8.34(3)	1.43(2)
			6800	8.12(5)	1.34(2)
45888	6.3741	0.94678	1500	5.88(3)	1.68(4)
			5400	6.06(3)	1.08(2)
			10800	5.91(3)	1.03(1)

method (an example of the RCA method). For real data, the WLS method yielded the most precise estimates. An advantage to using the WLS method is that Q and f_0 estimates have less variability than the other methods even for “noisy” resonance curves. (“Noisy” data can occur due to inadequate signal averaging and/or low coupling.) For one observed resonance curve, the 3-dB method does not provide an associated uncertainty for Q and f_0 whereas the WLS method does.

Given that the resonance curve was sampled at a fixed number of equally spaced frequencies in the neighborhood of the resonant frequency, we determined the optimal frequency spacing in order to minimize the asymptotic standard deviation of the estimate of either Q or f_0 . For optimal estimation of Q , with our experimental data, $\Delta = Q(f_{\max}/f_0 - 1) \approx 2.6$, where f_{\max} is the largest frequency. For optimal estimation of f_0 , $\Delta \approx 0.6$. The fractional uncertainty of f_0 is smaller than the fractional uncertainty of Q when mode interference is neglected.

APPENDIX A ESTIN METHOD

If additive noise and background are neglected, the resonance curve model can be written as

$$T_m(f_k) = \frac{T(f_0)}{1 + Q^2 \left(\frac{f_k}{f_0} - \frac{f_0}{f_k} \right)^2}.$$

A good approximation for high Q values is

$$2Q \left(\frac{f_k - f_0}{f_0} \right) \cong \left| \frac{T_m(f_0)}{T_m(f)} \right|^{1/2}.$$

At the k th frequency, define

$$x_k = \frac{2(f_k - \hat{f}_0)}{\hat{f}_0},$$

and

$$y_k = \left| \frac{T_m(f_0)}{T_m(f_k)} \right|^{1/2}.$$

Define

$$\hat{y}_k = \alpha_1 x_k + \alpha_2.$$

The values of α_1 and α_2 that minimize

$$\sum |y_k - \hat{y}_k|^2$$

are called $\hat{\alpha}_1$ and $\hat{\alpha}_2$. The Estin estimator of Q is $\hat{\alpha}_1$ [1].

APPENDIX B THE 3-dB METHOD

Define

$$r_{dB}(\Delta f) = 10 \log_{10} \left[\frac{T(\hat{f}_0)}{T(\hat{f}_0 + \Delta f)} \right].$$

Define Δf^+ to be the positive value of Δf such that $r_{dB}(\Delta f^+) = 3$, and Δf^- to be the negative value of Δf such that $r_{dB}(\Delta f^-) = 3$. According to the 3-dB method, we have

$$\hat{Q} = \frac{\hat{f}_0}{[\Delta f^+ - \Delta f^-]}.$$

If there is no measurement at the frequencies corresponding to $r_{dB}(\Delta f^+) = 3$ or $r_{dB}(\Delta f^-) = 3$, Δf^+ or Δf^- is estimated by a linear interpolation method.

APPENDIX C

VARIANCE FUNCTION DERIVATION: SPECIAL CASE

The quantity $T(f_k)$ is the sum of the squared real and imaginary components of the complex scattering parameter $S_{21}(f_k)$. The measured resonance curve can be expressed as

$$T_m(f_k) = [g(f_k) + e_{gk}]^2 + [h(f_k) + e_{hk}]^2 \quad (23)$$

where $g(f_k) = \Re[S_{21}(f_k)]$ and $h(f_k) = \Im[S_{21}(f_k)]$. The measured real and imaginary components of $T_m(f_k)$ are assumed to be statistically independent realizations of the same Gaussian process that has an expected value of 0 and variance σ^2 . Thus, at the k th frequency, the expected value of $T_m(f_k)$ is

$$E[T_m(f_k)] = g^2(f_k) + h^2(f_k) + 2\sigma^2 \quad (24)$$

and the variance of $T_m(f_k)$ is

$$\text{VAR}[T_m(f_k)] = 4\sigma^2[g^2(f_k) + h^2(f_k)] + 8\sigma^4. \quad (25)$$

Since $T(f_k) = g(f_k)^2 + h(f_k)^2$, then

$$E[T_m(f_k)] = T(f_k) + 2\sigma^2 \quad (26)$$

and

$$\text{VAR}[T_m(f_k)] = 4\sigma^2 T(f_k) + 8\sigma^4. \quad (27)$$

For this special case, (26) and (27) are consistent with (13) and (14) as

$$E[T_m(f_k)] = T(f_k) + BG \quad (28)$$

and

$$\text{VAR}[T_m(f_k)] = \frac{\gamma_1^2}{1 + Q^2 \left(\frac{f_k}{f_0} - \frac{f_0}{f_k} \right)^2} + \gamma_2^2 \quad (29)$$

where

$$\begin{aligned} BG &= 2\sigma^2 \\ \gamma_1^2 &= 4\sigma^2 T(f_0) \end{aligned}$$

and

$$\gamma_2^2 = 8\sigma^4.$$

REFERENCES

- [1] A. J. Estlin and M. D. Janezic, "Improvements in dielectric measurements with a resonance cavity," in *Proc. 8th IEEE Instrumentation and Measurement Technology Conf.*, 1991, pp. 573-579.
- [2] T. Miura, T. Takahashi, and M. Kobayashi, "Accurate q -factor evaluation by resonance curve area methods and its applications to the cavity perturbation," *IEICE Trans. Electron.*, vol. 6, pp. 900-907, 1994.
- [3] P. J. Petersen and S. M. Anlage, "Measurement of resonant frequency and quality factor of microwave resonators: Comparison of methods," *J. Appl. Phys.*, vol. 84, no. 5, pp. 3392-3402, 1998.
- [4] M. Davidian and R. J. Carroll, "Variance function estimation," *J. Amer. Stat. Assoc.*, vol. 82, no. 400, pp. 1079-1092, 1987.
- [5] E. L. Ginzton, *Microwave Measurements*. New York: McGraw-Hill, 1957.
- [6] C. G. Montgomery, R. H. Dicke, and E. M. Purcell, *Principles of Microwave Circuits*. New York: McGraw-Hill, 1974.
- [7] D. Kajfez, "Q factor," in *Vector Fields*. Oxford, MS: Oxford, 1994.
- [8] Y. Bard, *Nonlinear Parameter Estimation*. New York: Academic, 1974.
- [9] D. M. Gay, "Computing optimal locally constrained steps," *SIAM J. Sci. Stat. Comput.*, vol. 2, pp. 186-197, 1981.
- [10] R. J. Cook, "Microwave cavity methods," in *High Frequency Dielectric Measurement*, J. Chamberlain and G. W. Chantry, Eds. Guildford, U.K.: IPC Sci. Technol. Press, 1973, pp. 12-27.
- [11] E. Ni and U. Stumper, "Permittivity measurements using a frequency-tuned microwave TE₀₁ cavity resonator," in *Proc. Inst. Elect. Eng.*, vol. 132, Feb. 1985, pp. 27-32.

Kevin J. Coakley received the Ph.D. degree in statistics from Stanford University, Stanford, CA, in 1989.

He is currently a Mathematical Statistician with the National Institute of Standards and Technology, Boulder, CO. His research interests include statistical signal processing, computer intensive statistical methods, and planning and analysis of experiments in physical science and engineering.

Jolene D. Spiett received the B.S. degree in mathematics/statistics and the M.S. degree in statistics from the University of Wyoming, Laramie.

She is a Mathematical Statistician with the Statistical Engineering Division, National Institute of Standards and Technology (NIST), Boulder, CO, where her primary duty is to provide general statistical support for the scientists and engineers of NIST.

Michael D. Janezic (M'91-SM'02) received the B.S. and M.S. degrees in electrical engineering from the University of Colorado at Boulder, in 1991 and 1996, respectively, and is currently working toward the Ph.D. degree in electrical engineering in the area of electromagnetic theory at the University of Colorado at Boulder.

In 1988, he joined the Radio Frequency Technology Division, National Institute of Standards and Technology (NIST), Boulder, where he has primarily focused on the development of techniques for measuring the broad-band electrical properties of dielectric substrates and thin films.

Raian F. Kaiser received the B.S.-E.E./C.S. degree from the University of Colorado at Boulder, in 1986.

He is currently with the Electromagnetic Properties of Materials Group, National Institute of Standards and Technology, Boulder, CO.